

Lucius Pitkin
INCORPORATED



Metallurgical and Chemical Consultants
Testing Laboratories-Nondestructive Examination Services

50 HUDSON STREET, NEW YORK, N.Y. 10013 · (212) 233-2737
TELEX 12-6615 · CABLE NIKTIP · (212) 233-2558

TECHNICAL REPORT NO. 7164

METALLURGICAL EXAMINATION OF SHELL
GIRTH WELD COUPON FROM
STEAM GENERATOR 32
INDIAN POINT 3
NUCLEAR POWER PLANT

PREPARED BY

A. J. VECCHIO, P.E.
VICE PRESIDENT & ASST. CHIEF METALLURGIST

PREPARED FOR

POWER AUTHORITY OF THE STATE OF NEW YORK
10 COLUMBUS CIRCLE
NEW YORK, NEW YORK

OCTOBER 19, 1982

8211220397 821117
PDR ADOCK 05000286
P PDR

Lucius Pitkin incorporated

TABLE OF CONTENTS

	<u>Page No.</u>
I. SUMMARY - - - - -	1
II. INTRODUCTION - - - - -	4
III. SHELL GIRTH WELD COUPON - - - - -	6
A. Visual Examination - - - - -	6
B. Magnetic-Particle Examination - - - - -	6
C. Radiographic Examination - - - - -	7
D. Ultrasonic Examination - - - - -	7
E. Deep-Etch Examination - - - - -	8
F. Composition - - - - -	10
G. Mechanical Properties	
1. Brinell Hardness - - - - -	11
2. Microhardness - - - - -	11
3. Tensile Test - - - - -	13
4. Charpy Impact Test - - - - -	14
5. J Integral Fracture Toughness Testing - -	15
H. Fractographic Examination - - - - -	17
I. Fracture Surface Analysis - - - - -	18
J. Metallographic Examination - - - - -	19
IV. DISCUSSION AND CONCLUSIONS - - - - -	23

Appendix

Tables I through IV

Figs. 1 through 47

Lucius Pitkin
i n c o r p o r a t e d

-1-

I. SUMMARY

A metallurgical investigation of in-service shell cracking in Indian Point 3 Nuclear Power Plant (IP3-NPP) steam generator 32 was performed. The investigation was carried out on a 6-inch diameter coupon removed from the upper shell-transition cone girth weld which contained several cracks. In addition to the sustained cracks, the coupon contained a discontinuity that extended completely through the wall thickness.

The program of investigation included fluorescent magnetic-particle, ultrasonic and radiographic examination followed by in-depth fractographic and metallographic examination, chemical and energy dispersive X-ray analyses, and mechanical and fracture toughness testing of shell and girth weld material.

Investigation showed the steam generator shell cracking to have initiated from the inner surface and to be associated with fine pits. The mode of cracking was found to be transgranular and, considering the association with pitting corrosion and manner of penetration, characteristic of corrosion enhanced progressive cracking - "corrosion fatigue".

**Lucius Pitkin
incorporated**

-2-

Fracture toughness testing revealed the upper shell, transition cone and weld deposit materials all to exhibit high toughness indicating a substantial tolerance for crack extension before final rupture.

The girth weld heat-affected zone hardness was considered inordinately high at Rockwell C 39 to 41 and, in our opinion, was indicative of less-than-satisfactory stress relief heat treatment.

The through-wall thickness discontinuity in the girth weld, which leaked in service, appeared to be the result of the propagation of one or more cracks in a vertical plane with respect to the vertical axis of the generator. Propagation of the crack to the outer surface of the shell allowed high pressure steam/water environment to escape and to erode the shell material along the crack front producing a vertically oriented, elongated hole on the outer surface.

Based upon the nature and extent of cracking as represented in the girth weld coupon, it appears that cracking is attributable primarily to high residual stresses and normal cyclic stresses incurred during operation and nucleated at sites of mild corrosion pitting attack of the weld and adjacent shell material. The role of residual stress in crack nucleation is difficult to assess, however, high residual tensile stresses would be detrimental with respect to initiation of cracks. It

**Lucius Pitkin
incorporated**

-3-

is generally accepted that once nucleated, crack propagation is governed by the magnitude of the cyclic stress range when maximum stresses are below the yield point. Further, the rate of crack propagation is significantly influenced by the environment.

**Lucius Pitkin
incorporated**

-4-

II. INTRODUCTION

A 6-in. diameter coupon removed from steam generator 32, IP3-NPP was submitted to Lucius Pitkin, Inc. for metallurgical investigation. The generator was manufactured by Westinghouse Electric Corporation and had approximately three years of effective full power operation from 1976 to 1982 when a leak was detected at a girth weld.

The nuclear steam electric generating unit is a 3025 MWT PWR system incorporating four Westinghouse Series 44 vertical U-tube steam generators. The secondary side of the steam generators operate at approximately 755 psig and 515 F at full load.

We were advised that the shell of steam generator 32 had sustained a leak in the circumferential or girth weld joining the upper shell to the transition cone. Subsequent non-destructive examination revealed the presence of numerous, generally circumferentially and a few vertically and obliquely oriented cracks on the inner surface in and about the weld. The inner surface of the shell in the area of the girth weld also exhibited numerous fine corrosion pits. Similar inner surface cracks and pitting were also observed in the area of the same girth weld in the other three steam generators.

**Lucius Pitkin
incorporated**

-5-

The through-wall thickness leak had manifested itself on the outer surface in the form of an elongated hole measuring approximately 3/16 inch wide by 5/8 inch long. It was from the area containing the discontinuity and associated inner surface cracks that the 6-in. diameter coupon was removed. The coupon was removed by drilling a series of overlapping holes around a 6-in. diameter circumference with the discontinuity at the center. The location of the steam generator shell girth weld from which the coupon was taken is shown in Fig. 1.

**Lucius Pitkin
incorporated**

-6-

III. SHELL GIRTH WELD COUPON

A. Visual Examination

The 6-in. diameter shell girth weld coupon, Figs. 2 to 4, forwarded to Lucius Pitkin, Inc. presented a relatively clean appearance free of any significant corrosion product on the inner or outer surface. The inner surface exhibited numerous fine, oxide-filled corrosion pits and several cracks generally oriented circumferentially, as shown in Figs. 5 and 6. The through-thickness elongated hole had its long axis parallel to the vertical axis of the steam generator. The periphery of the hole, as seen in Fig. 7, was smooth as would occur from erosion by escaping steam. A fine, 1/2-in. long vertical crack extended from the lower end of the elongated hole. No other cracks were present on the outer surface.

B. Magnetic-Particle Examination

The drill hole ridges present on the periphery of the coupon were uniformly ground to provide a smooth surface for nondestructive examination. The ground coupon was subjected to fluorescent magnetic-particle inspection. Numerous crack indications were found on the inner surface, three of which intersected the periphery of the coupon. Figs. 8 and 8A show the indications observed under ultraviolet

Lucius Pitkin
incorporated

-7-

light. Fluorescent magnetic-particle examination of the outer surface revealed a fine, vertically oriented crack emanating from the lower end of the through-thickness discontinuity. No other indications were observed on the outer surface. Fig. 9 and 9A show the crack indication observed under ultraviolet light on the outer surface of the girth weld coupon.

C. Radiographic Examination

Radiographic examinations of the coupon using a Cobalt 60 source, at a source to film distance of 15 in., revealed the inner surface cracks to have propagated to varying depths. Further, it appeared that one and possibly two of the inner surface cracks had intersected the through-wall discontinuity.

D. Ultrasonic Examination

The coupon was ultrasonically examined using 1 MHz and 2-1/4 MHz normal and shear wave transducers over all surfaces. Results of the ultrasonic examination confirmed that several of the inner surface cracks had attained a significant depth and that at least two of the cracks near the inner surface were associated with the through-thickness discontinuity.

Lucius Pitkin
incorporated

-8-

Fig. 10 is a sketch showing the results of the various non-destructive examinations performed on the coupon.

E. Deep-Etch Examination

Before deep-etch examination, in order to maintain orientation with respect to the vertical axis of the steam generator, the coupon was stamped so that the shell was at zero degrees (vertically up) and the transition cone at 180 degrees (vertically down).

Light etching of the periphery of the coupon revealed the presence of a major weld repair at the root or inner surface of the circumferential weld. The weld repair, which was about 1-1/2 in. deep by 2 in. wide, was confined to the transition cone and extended across the diameter of the coupon. Figs. 11 through 14 are photomicrographs showing the periphery of the lightly etched coupon at 90-degree intervals. One of the the inner surface cracks which had extended into the periphery of the coupon is shown in Fig. 15.

The coupon was cross-sectioned diametrically in a vertical direction; that is, 0 to 180 degrees with respect to the axis of the steam generator. The mating cut surfaces were ground and lightly etched to reveal the general macrostructure of the girth weld and the depth of the intersected inner surface cracks. It was observed that cracking

Lucius Pitkin
i n c o r p o r a t e d

-9-

occurred in the repair weld in the transition cone and in the upper shell base material. The mating etched diametrical cross-section surfaces are shown in Figs. 16 and 17, respectively.

One of the coupon halves was retained for preparation of J-integral fracture toughness and fatigue tests; the other half was sectioned approximately 5/8 in. from and parallel to the previous diametrical cut so as to include the elongated hole on the outer surface. This longitudinal cross-section was ground flat and lightly etched.

Examination of the etched cross-section revealed the presence of a somewhat irregular crack that extended from the toe of the inner surface repair weld into the crown weld at approximately mid-wall where it then joined an eroded area approximately 3/8 in. wide along the line of fusion between weld deposit and upper shell. This is shown in Fig. 18.

The etched cross-section, shown in Fig. 18, was re-ground an additional 0.060 in. so as to further assess the extent of cracking and nature of the through-wall discontinuity. It was observed that the crack emanating from the inner surface and the through-wall thickness discontinuity contained deposits of what appeared to be oxide, metallic copper and a fibrous, wood-like material. We were advised that the

Lucius Pitkin
i n c o r p o r a t e d

-10-

fibrous material was the remnants of a wood plug inserted into the hole by plant personnel after the unit was placed in cold shutdown. No evidence of charring or coking was associated with the wood-like material. Fig. 19 is a photomicrograph showing the ground surface. Figs. 20 through 23 are color photographs showing the longitudinal section containing the through-thickness discontinuity.

F. Composition

Qualitative spectrographic and quantitative chemical analyses of drillings taken from the upper shell, transition cone, crown weld and repair weld of the submitted coupon. The analyses revealed the upper shell and transition cone base metal to be similar in composition, both corresponding to a modified ASME SA 302B material.

Analyses further revealed the crown and repair welds also to be similar in composition, with the crown weld exhibiting a somewhat higher carbon content than the repair weld. The crown and repair weld were similar in composition to E8018-C3 nickel steel electrode (SFA-5.5).

Complete results of the analyses performed are given in Tables I and II.

Lucius Pitkin
incorporated

-11-

G. Mechanical Properties

1. Brinell Hardness

Brinell hardness surveys were performed on a ground longitudinal cross-section of the steam generator coupon. The surveys showed the upper shell and transition cone base materials to exhibit a uniform hardness of Brinell 190 to 200. The crown weld exhibited a uniform Brinell hardness of 210 to 230. The repair weld exhibited a uniform hardness of Brinell 190 to 200. A survey of the heat-affected zone between the upper shell/crown weld, transition cone/crown weld and the transition cone/repair weld showed the heat-affected zones to be significantly harder at Brinell 240 to 255.

Location and results of the Brinell hardness surveys are shown in Fig. 24.

2. Microhardness

A microhardness survey using a Knoop indenter at 500 gram load was performed on longitudinal specimens containing the crown weld/upper shell and crown weld/transition cone heat-affected zones. These specimens were taken to include the outer surface at the weld

Lucius Pitkin
i n c o r p o r a t e d

-12-

toes. A third specimen was taken from the repair weld/transition cone near the inner surface.

Results of the Knoop microhardness survey showed the heat-affected zone in the three areas to be inordinately high at KHN 390 to 425. This converts to Rockwell C 39 to 42. The high hardness exhibited by the girth weld heat-affected zone is indicative of insufficient stress relief which would also imply the presence of residual stresses (see Fig. 25).

In order to assess the temperature of stress relief heat treatment, specimens from the upper shell/crown weld and transition cone/crown weld cut from locations similar to where the microhardness survey specimens were obtained, were heat treated at 1000 and 1100 F for 1 hour each. The results of microhardness survey on this re-heat treated material showed heat-affected zone hardness to be reduced to Rockwell C 30 to 32 after exposure at 1000 F and to Rockwell C 28 to 29 after exposure at 1100 F. The results of these heat treatment tests indicate that the subject girth weld had been stress relieved at a temperature of less than 1000 F in the areas where the hardness measurements were made.

Location and results of the microhardness surveys are shown in Fig. 25. The heat-affected zone microstructure for the

Lucius Pitkin
incorporated

-13-

as-received coupon specimen , 1000 F and 1100 F laboratory heat-treated coupon specimens are shown in Figs. 25A, 25B and 25C.

3. Tensile Test

A sub-size, 0.357-in. diameter tensile specimen was prepared from the upper shell generator material in the through-thickness direction. (This test direction usually shows lower properties with respect to the standard longitudinal direction.)

Results of the tensile test shown below indicate the material to meet the longitudinal tensile requirements for SA 302, Grade B material.

Lucius Pitkin
incorporated

-14-

	<u>SA 302 Grade B</u>	<u>Upper Shell</u>
Ultimate tensile strength, psi	80,000-100,000	86,300
Yield strength, 0.2% offset	50,000 min.	67,000
Elongation, % in 2.0 in.	18	21.0*

*1.4 in. gage length

4. Charpy Impact Tests

Standard Charpy V-notch specimens were prepared from the upper shell, transition cone, crown weld, repair weld, heat-affected zone between the upper shell/crown weld and heat-affected zone between transition cone/crown weld material. Specimen lengths were oriented parallel to the vertical axis of the steam generator; the V-notch was oriented circumferentially facing the inner surface side of the generator shell so as to reflect the orientation of observed crack growth.

Lucius Pitkin
incorporated

-15-

All the Charpy V-notch specimens were tested at 76 F and exhibited relatively high absorbed energies ranging from 60 to 111 ft-lb as is characteristic of tough materials.

Complete results of the Charpy impact tests are given in Table III.

5. J-Integral Fracture Toughness Testing

J-integral tests were conducted in order to ascertain the elastic-plastic fracture characteristic of the shell material of the steam generator. Values for J (in-lb/in²), the corresponding value of K (ksi $\sqrt{\text{in.}}$), and the crack extension Δa (in.) were determined using the single specimen unloading compliance technique in accordance with ASTM Standard E: 813-81. Sub-size, compact tension specimens were machined from the upper shell, crown weld, repair weld and cone regions of the coupon.

Results of the J-integral tests are presented in Table IV. The values obtained are not valid J_{IC}/K_{IC} results. Invalid J_{IC}/K_{IC} results were due to large differences between the total crack extension measured by the unloading compliance technique and the actual crack extension measured after heat tinting. Nevertheless, for all specimens tested, except CW1J, a significant amount of crack

Lucius Pitkin
incorporated

-16-

extension and high values (greater than 170 ksi $\sqrt{\text{in.}}$) of fracture toughness were measured. Specimen CWLJ from the crown weld/repair weld interface, exhibited only a small amount of crack extension, as compared to the other specimens, prior to final failure. However, CWLJ did reach a J value of 1087 in-lb/in² (a maximum K of 180 ksi $\sqrt{\text{in.}}$) indicating relatively good toughness.

There was some irregularity noted in the pre-cracking preparation of specimen CWLJ which indicated the probable presence of residual stresses. A residual stress field may also have contributed to a less tough behavior of this specimen as compared to the other specimens.

Specimens from the upper shell were tested at room temperature and at 500 F. The J values measured at these temperatures were comparable (997 in-lb/in² @ room temperature and 1156 in-lb/in² @ 500 F), however, the specimen tested at 500 F exhibited a lower resistance to tearing.

In general, all the materials tested exhibited high levels of fracture toughness and indicate a high tolerance for a significant amount of crack extension before final rupture.

Lucius Pitkin
i n c o r p o r a t e d

-17-

6. Fatigue Tests

Fatigue specimens are presently being prepared for testing in the steam generator secondary water environment. Results are not yet available at this time the report was prepared.

H. Fractographic Examination

The test coupon was cut so as to intercept the weld and base metal cracks. Forced separation of a crack revealed the fracture surface to be generally smooth in appearance and to contain a thumbnail-size zone with radially oriented ridges and faint beach-like markings originating from a pit at the inner surface as is characteristic of progressive cracking. Fig. 26 is a close-up photograph showing the crack surface at the origin site at the inner surface of the coupon.

Scanning electron microscopy at the origin site of the crack surface shown in Fig. 26 revealed the presence of a corrosion product and confirmed the pitting corrosion attack at the origin site. Fig. 27 is a scanning electron micrograph of the origin site. The presence of corrosion products on the crack surface precluded the observance of striation lines. At higher magnification, the presence of discrete crystals of iron oxide was observed. These crystals are shown in Fig. 28.

Lucius Pitkin
i n c o r p o r a t e d

-18-

Further examination by scanning electron microscopy of the fracture surface below the origin revealed in addition to the presence of corrosion product that the fracture surface was somewhat radially ridged from the origin suggesting the fracture to be the result of progressive or fatigue cracking. The corroded fracture surface and radial ridges that emanated from the origin is shown in Fig. 29.

Extensive cleaning of the fracture surface removed some of the oxide corrosion product. However, striation lines were not found (and would not be expected to be found, although the attempt made, because of the corrosion that occurred). The cleaned fracture surface is shown in Fig. 30.

All of the other crack surfaces examined, whether through base metal or weld deposit, exhibited similar characteristics.

I. Fracture Surface Analysis

Energy dispersive X-ray analysis (EDAX) was performed on fracture surface areas of opened-up cracks. The EDAX spectrum obtained from weld and base metal cracks showed energy peaks for aluminum, manganese, iron, nickel, copper and zinc. The iron, manganese and nickel are attributable to the base metal. The presence of copper, aluminum and zinc is attributable to carry-over from copper alloy

Lucius Pitkin
incorporated

-19-

components in the secondary system. Fig. 31 is a photograph showing a typical EDAX spectrum obtained.

(Previously, LPI had performed Auger analysis on fracture surface area of a crack in a boat sample removed from the same girth weld of steam generator 32 (see our Report M-6785, T.R. 7154 dated June 24, 1982). This analysis revealed the elements silicon, sulfur, chlorine, carbon, nitrogen, oxygen, iron, copper and sodium.)

J. Metallographic Examination

Several microspecimens were cut from the coupon so as to intersect the inner surface cracks that extended through weld and base metal.

In the as-polished, unetched condition, whether in weld or base metal, no unusual quantities of non-metallic inclusions were observed. Several, fine secondary cracks were observed emanating from pits at the inner surface. These cracks were generally corrosion filled and relatively straight as is characteristic of corrosion enhanced progressive cracking in the nature of fatigue. Without exception, all of the cracks had initiated on the inner surface of the coupon.

Lucius Pitkin
i n c o r p o r a t e d

-20-

Etching of the specimens revealed that the cracking through the heat-affected zone and base material was transgranular and slightly branching. Fig. 32 is a photomicrograph showing one of the typical progressive or fatigue cracks initiated near the toe of the repair weld propagating into the transition cone base material. Figs. 33 through 36 are photomicrographs, at higher magnification, showing the progression of the cracks from the inner surface near the toe of the repair weld into the transition cone base metal. It was also observed that the cracks contained a significant quantity of metallic copper.

Similarly, Figs. 37 through 39 are photomicrographs at high magnification showing the penetration of fine, oxide-filled cracks penetrating from pits at the inner surface of the transition cone base metal adjacent to the repair weld. Examination revealed the presence of fine pits on the inner surface near the heat-affected zone which were free of any cracks as shown in Fig. 39A.

Examination of the weld heat-affected zones, both crown and repair, revealed the heat-affected zone microstructure to consist of coarse, lightly tempered martensite as illustrated in Figs. 40 and 41.

In order to better evaluate the nature of the through-wall discontinuity, as shown in Fig. 41, specimens were cut from the etched macrostructure perpendicular to the discontinuity at five different wall

Lucius Pitkin
incorporated

-21-

depth levels. These specimens were prepared for metallographic examination.

Examination of the specimens revealed the through-wall discontinuity (evidenced on the outer surface) to have been a vertically oriented crack which had progressed from a horizontal crack at the inner surface through the entire wall thickness. The location of this crack with respect to the through-wall discontinuity is shown in Figs. 43 and 44.

Examination of the five specimens (A through E) intersecting the through-wall discontinuity did not reveal the presence of any associated slag, porosity or other weld defects. No evidence of carbon depletion as might occur from high temperature exposure during stress relieving was observed. The crack was found to be transgranular as were all the cracks observed whether through weld, heat-affected zone or base metal. The crack was corrosion filled and found to contain significant quantities of metallic copper. Based upon this extensive examination, it appeared that the through-wall discontinuity was the result of an initially circumferentially oriented crack which had initiated on the inner surface and had progressed under cyclic loading. Apparently, in the area of the repair weld, the crack had turned from a horizontal to a vertical direction as a result of the influence of residual stresses

Lucius Pitkin
incorporated

-22-

while propagating through the wall thickness. When the crack had reached the outer surface of the wall, erosion by escaping steam and water produced the wide, vertically oriented gap or hole.

Fig. 45 is a photomicrograph showing the oxide-filled crack exhibited by specimen C, shown in Fig. 43. The corrosion-filled crack also contains particles of copper. Fig. 46 is a photomicrograph showing the heat-affected zone in specimen D, shown in Fig. 44. Fig. 47 is another photomicrograph showing the cracking associated with the through-wall discontinuity. In all cases, no welding defects of any type were observed.

Lucius Pitkin
incorporated

-23-

IV. DISCUSSION AND CONCLUSIONS

Metallurgical evaluation of the upper shell-to-transition cone girth weld identified the mode of cracking to be transgranular and characteristic of corrosion-enhanced progressive cracking in the nature of fatigue. All of the cracks examined regardless of location or orientation, i.e., upper shell, transition cone, crown weld, or repair weld, were transgranular, slightly branched and totally or partially filled with corrosion product and usually initiated from a fine pit on the inner surface. Analysis of the deposits within the cracks indicated the deposits to consist of metal oxides, primarily iron oxide. The presence of metallic copper was also observed in all the cracks examined.

No evidence of weld defects such as slag, porosity, or decarburization was associated with the through-wall vertically oriented crack or with any of the cracks which had partially penetrated the vessel wall. The absence of decarburization associated with crack surfaces indicates the high probability that these cracks did not occur as a result of welding.

The significantly high heat-affected zone hardness (Rockwell C 39 to 41) of the crown and repair welds and the lower hardness exhibited by heat-affected zone specimens after laboratory heat treating (1000 F

**Lucius Pitkin
incorporated**

-24-

and 1100 F for 1 hr.) implies the presence of commensurately high residual stresses in the girth weld that had not been relieved by the post-weld stress-relief heat treatment applied in fabrication of the joint.

The final vertical orientation of the through-wall crack at the outer surface as compared to the generally circumferential orientation at the inner surface, the same as the other girth weld cracks at the inner surface, is attributable to the crack propagating into a stress field of different orientation - particularly in the area of the major repair weld.

Initiation of the cracks at the inner surface and propagation into the vessel wall is attributed to high residual tensile stresses and normal cyclic service stresses aggravated by a small amount of pitting corrosion. The contribution of residual stresses in crack nucleation could not be quantified from the metallographic studies. However, initiation and changing of crack direction during propagation would be influenced by residual stress fields.

The fatigue crack growth rate is enhanced by corrosion when cyclic stresses are high and frequency of loading is low. The significant amount of metallic copper associated with the cracks corroborates the cyclic loading to be of low frequency, as the

Lucius Pitkin
incorporated

-25-

deposition of the copper deep within the cracks occurs over a long period of time.

With respect to the fracture toughness of the girth weld materials, it is evident that the vessel is capable of satisfying a "leak-before-break" criterion. That is, the critical crack size at the operating stress levels is greater than the wall thickness of the vessel so that failure occurs by crack penetration through the wall and the vessel leaks (as was the case for Steam Generator 32). Ultimately, continued operation with a through-wall crack that continues to grow could result in rupture of the vessel.

Lucius Pitkin
incorporated

APPENDIX

Lucius Pitkin

INCORPORATED



Metallurgical and Chemical Consultants

Testing Laboratories-Nondestructive Examination Services

50 HUDSON STREET, NEW YORK, N.Y. 10013 (212) 233-2737
TELEX 12-6615 CABLE NIKTIP (212) 233-2558

TABLE I
SPECTROGRAPHIC ESTIMATES

Report No. M-6855

Date October 18, 1982

The following is our analysis of 2 sample(s) ~~or~~ as indicated below

BY QUANTITATIVE CHEMICAL AND QUALITATIVE SPECTROGRAPHIC ANALYSES

	<u>Specified SA 302 Grade B</u>	<u>Upper Shell</u>	<u>Transition Cone</u>
Carbon, %	0.25 max.	0.24	0.23
Manganese	1.07	1.48	1.39
Phosphorous	0.035 max.	0.011	0.012
Sulfur	0.040 max.	0.019	0.015
Silicon	0.13-0.45	0.25	0.27
Molybdenum	0.41-0.64	0.51	0.49
Nickel	-	0.50	0.11
Chromium	-	0.11	0.11
Vanadium	-	Not found	Not found
Iron		Major	Major
Copper		0.0X low	0.0X low
Aluminum		0.0X low	0.0X low
Magnesium		0.00X low	0.00X low

Other elements looked for, but not found:

titanium, zirconium, zinc, bismuth, lead, tin, LUCIUS PITKIN, INC.
antimony, gallium, germanium, boron, cobalt, columbium,
tungsten, beryllium. ~~BY~~

NOTE: Major = above 5% estimated. Minor = 1.5% estimated. .X, .OX, .OOX, etc. = concentration of the elements estimated to the nearest decimal place - e.g. .OX = .01-.09% estimated. * = less than. NF = not found. The numbers in parenthesis indicate the estimated relative concentration of the element among the various samples. Detectability varies considerably among the elements and also depends upon the amount and nature of the sample, therefore, "Not Found" or NF means not detected in the particular sample by the technique employed.



TABLE II
SPECTROGRAPHIC ESTIMATES

Report No. M-6855

Date October 18, 1982

The following is our analysis of 2 sample(s) ~~as~~ as indicated below

BY QUANTITATIVE CHEMICAL AND QUALITATIVE SPECTROGRAPHIC
ANALYSES

	Specified SFA 5.5 (E8018-C3)	Crown Weld	Repair Weld
Carbon, %	0.12 max.	0.11	0.06
Manganese	0.40-1.25	1.37	0.98
Phosphorous	0.030 max.	0.017	0.014
Sulfur	0.030 max.	0.010	0.012
Silicon	0.80 max.	0.27	0.36
Nickel	0.80-1.10	0.64	1.08
Chromium	0.15 max.	0.045	0.050
Molybdenum	0.35 max.	0.42	0.24
Vanadium	0.05 max.	*0.01	*0.01
Iron		Major	Major
Copper		0.0X high	0.00X high
Aluminum		0.00X	0.00X
Magnesium		0.00X low	0.00X low

Other elements looked for, but not found:

titanium, zirconium, zinc, bismuth, lead, tin,
 antimony, gallium, germanium, boron, cobalt,
 columbium, tungsten, beryllium.

LUCIUS PITKIN, INC.

By

NOTE: Major = above 5% estimated. Minor = 1.5% estimated. .X, .OX, .OOX, etc. = concentration of the elements estimated to the nearest decimal place - e.g. .OX = .01-.09% estimated. * = less than. NF = not found. The numbers in parenthesis indicate the estimated relative concentration of the element among the various samples. Detectability varies considerably among the elements and also depends upon the amount and nature of the sample, therefore, "Not Found" or NF means not detected in the particular sample by the technique employed.

Lucius Pitkin
incorporated

TABLE III

GIRIH WELD COUPON
STEAM GENERATOR 32

CHARPY V-NOTCH TEST RESULTS

<u>Specimen Notch Location</u>	<u>Test Temp., °F</u>	<u>Energy Absorbed, ft-lbs.</u>	<u>Lateral Expansion</u>	<u>Percent Shear</u>
Transition Cone	76	79.0	0.063	85
Transition Cone	76	69.0	0.058	80
Upper Shell	76	77.0	0.067	95
Upper Shell	76	75.0	0.064	95
Crown Weld	76	60.0	0.051	60
Repair Weld	76	111.0	0.085	95
Crown Weld/Cone Heat-Affected Zone	76	83.0	0.059	90
Crown Weld/Cone Heat-Affected Zone	76	74.0	0.059	85
Crown Weld/Upper Shell Heat-Affected Zone	76	83.0	0.061	95
Crown Weld/Upper Shell Heat-Affected Zone	76	71.0	0.044	60

TABLE IV

GIRTH WELD COUPON - STEAM GENERATOR 32

SINGLE SPECIMEN J-INTEGRAL TEST DATA SUMMARY

SPECIMEN ID	MATERIAL	GR	E	YS	UTS	TEMP	TYPE	THICK	WIDTH	BO	BF	JFLD	JQ	JMAX	KFLD	KQ	POP	VALID
LP2	US1J	UPPER SHELL	30.0	70	100	69	CT	0.500	0.992	0.399	0.321	1414	997	3194	206	173	NO	NO
LP2	US2J	UPPER SHELL	30.0	70	100	500	CT	0.500	0.996	0.401	0.327	1244	1156	2125	193	186	NO	NO
LP2	RW1J	REPAIR WELD	30.0	70	100	69	CT	0.500	0.997	0.383	0.311	1152	1133	2315	186	184	NO	NO
LP2	C1J	CONE	30.0	70	100	69	CT	0.500	0.996	0.384	0.341	1237	1231	2326	193	192	NO	NO
LP2	CW1J	CROWN WELD	30.0	70	100	71	CT	0.500	0.992	0.383	0.177	1066	----	1087	179	--	YES	NO
LP2	CW2J	CROWN WELD	30.0	70	100	71	CT	0.497	0.994	0.381	0.332	1135	1308	2622	185	198	NO	NO

- E - Youngs Modulus, 10^6 psi
- YS - Yield strength, psi.
- UTS - Ultimate tensile strength, psi
- Temp.- Test temperature, F
- Type - Compact tension
- Thick- Specimen thickness, in.
- Width- Specimen width, in.
- BO - Ligament before J testing, in.
- BF - Ligament after J testing, in.
- JFLD - Value of J for first load drop, in-lb/sq.in.
- JQ - Tentative value for J, in-lb/sq.in.
- JMAX - Max. J for specimen, in-lb/sq.in.
- KFLD - Stress intensity value at first load drop, ksi $\sqrt{\text{in.}}$
- KQ - Tentative representative value, ksi $\sqrt{\text{in.}}$
- J integral - Toughness of material at onset of crack extension, in-lb/sq.in.

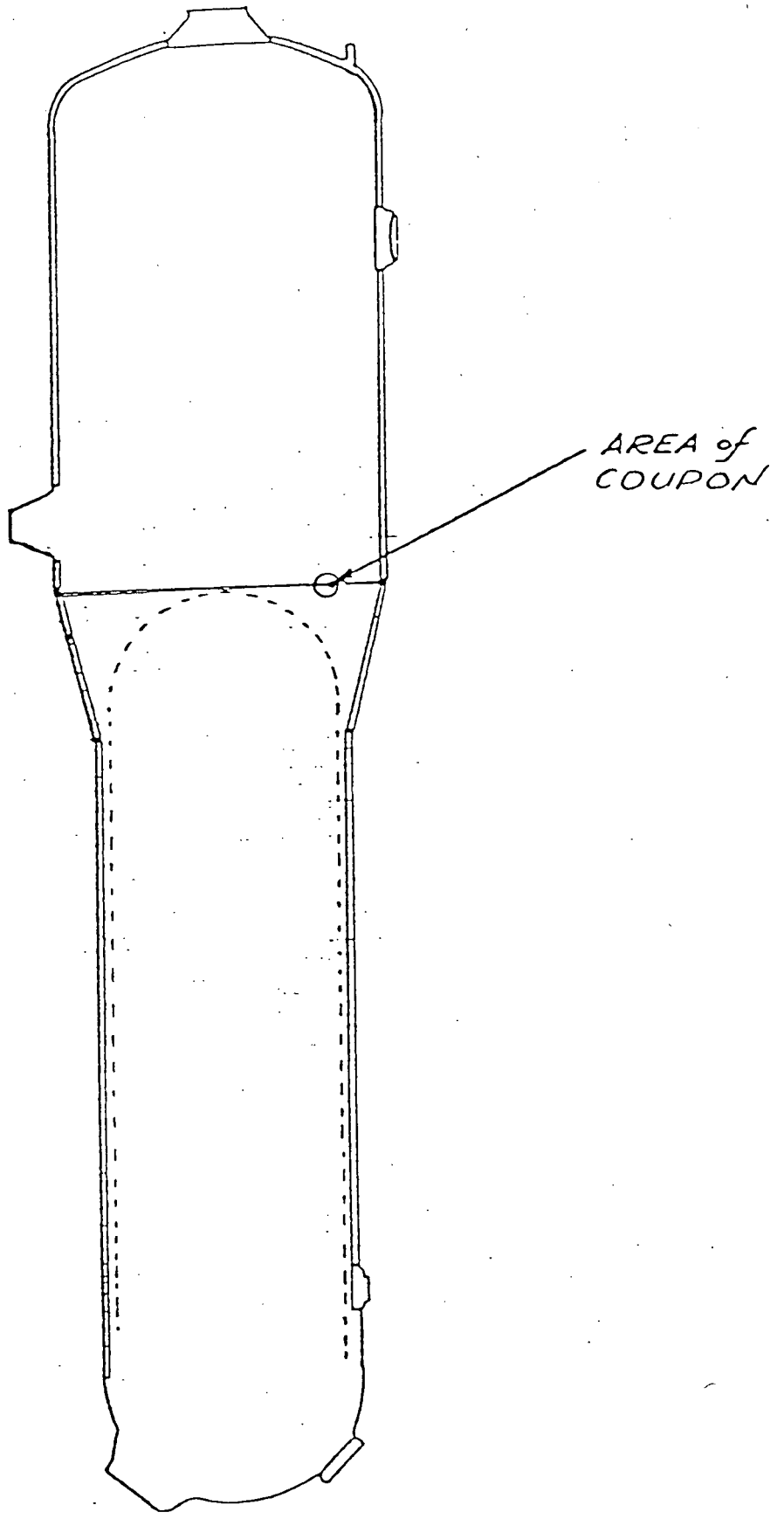


Fig. 1 LOCATION OF 6-INCH DIAMETER GIRTH WELD COUPON STEAM GENERATOR 32



Fig. 2 GIRTH WELD COUPON FROM STEAM GENERATOR 32,
AS-RECEIVED CONDITION

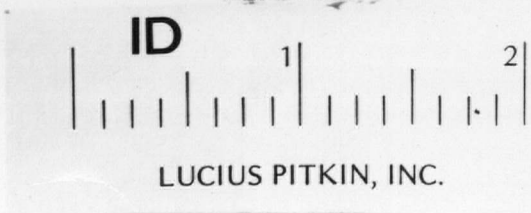
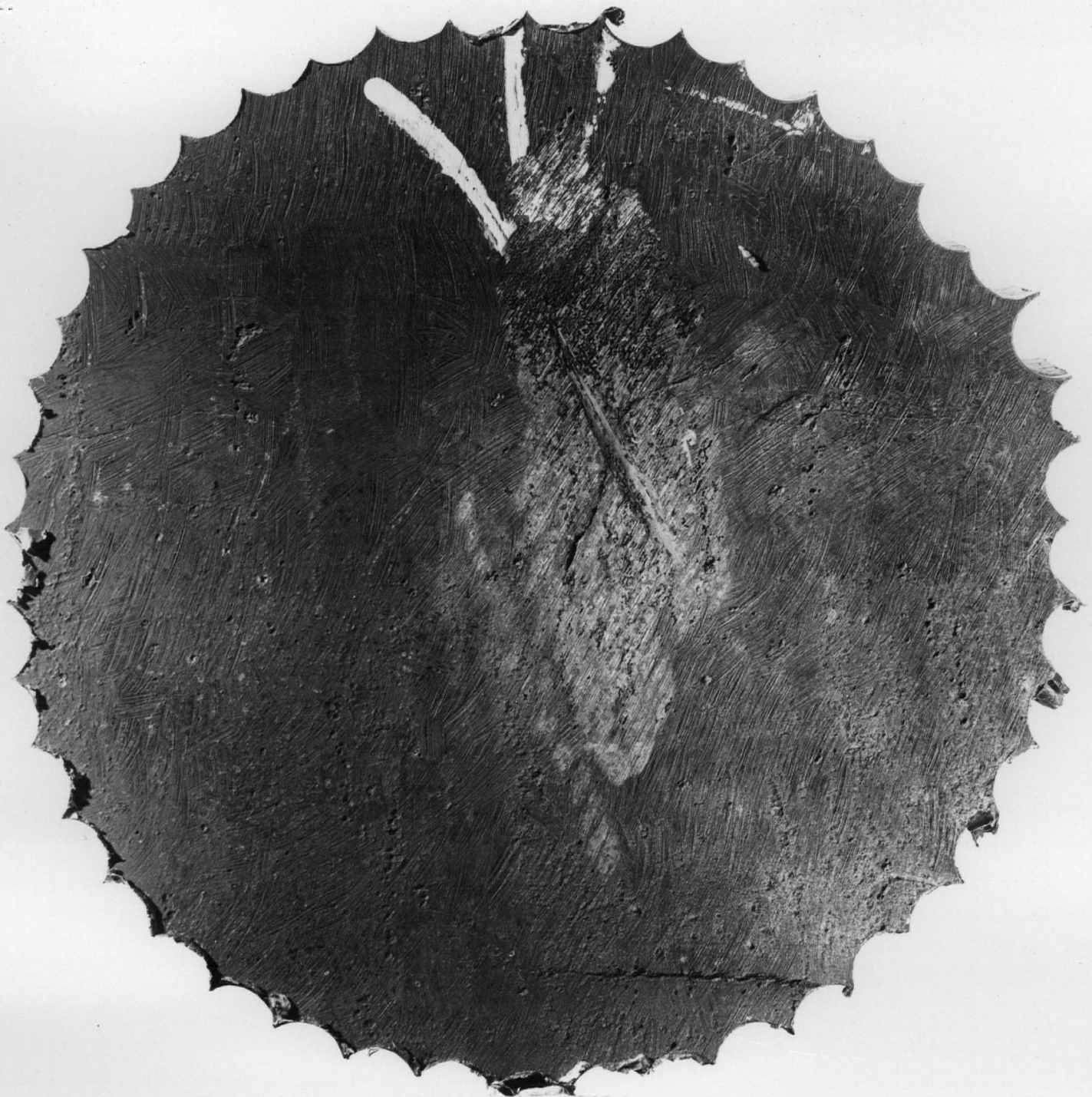
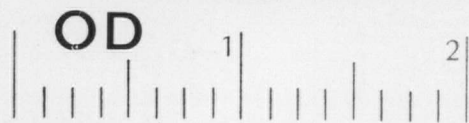
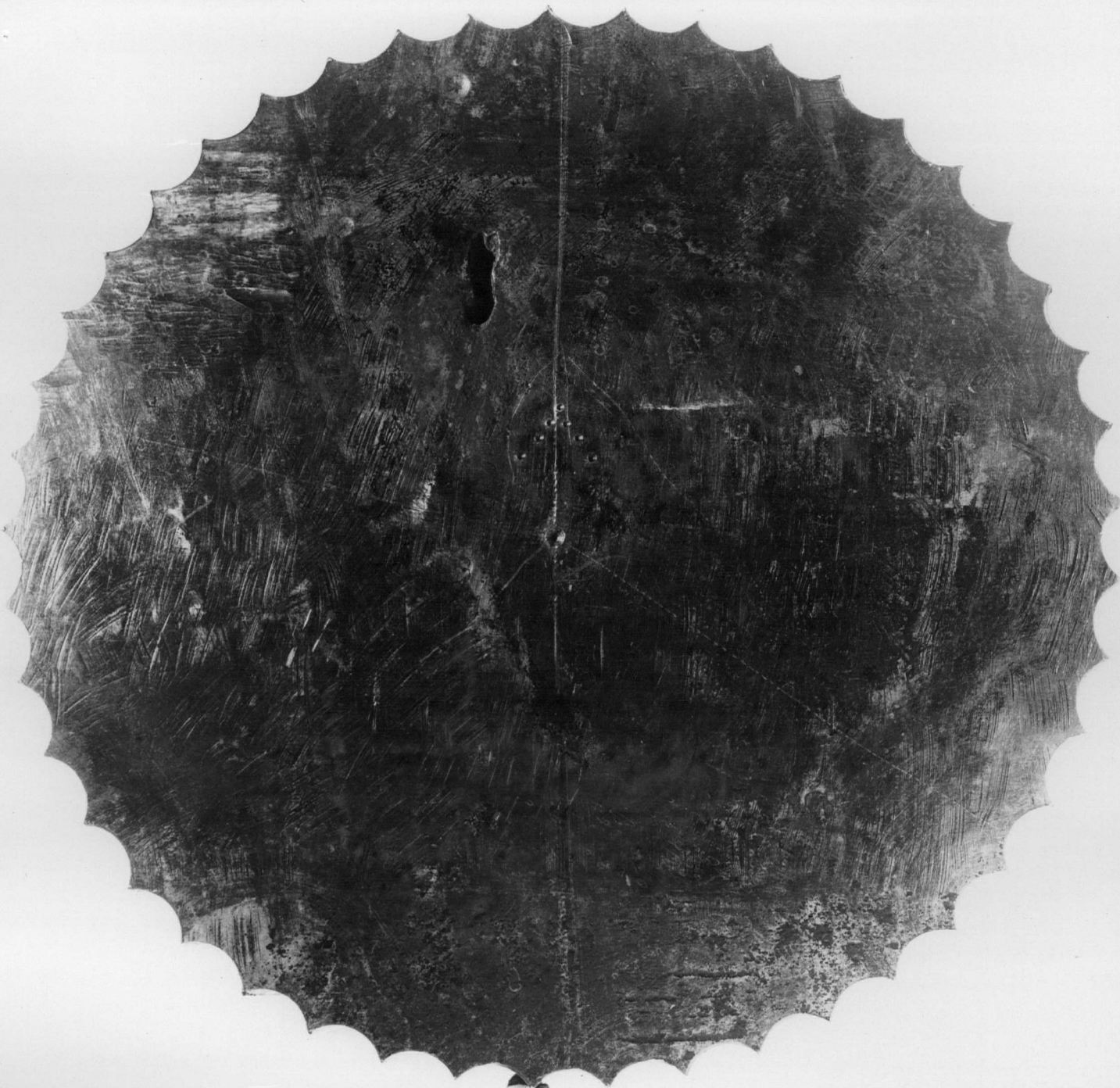


Fig. 3 GIRIH WELD COUPON - INNER SURFACE



LUCIUS PITKIN, INC.

Fig. 4 GIRTH WELD COUPON - OUTER SURFACE



ID

1

LUCIUS PITKIN, INC.

Fig. 5 INNER SURFACE CRACKS AND PITS



Fig. 6 INNER SURFACE CRACKS AND PITS

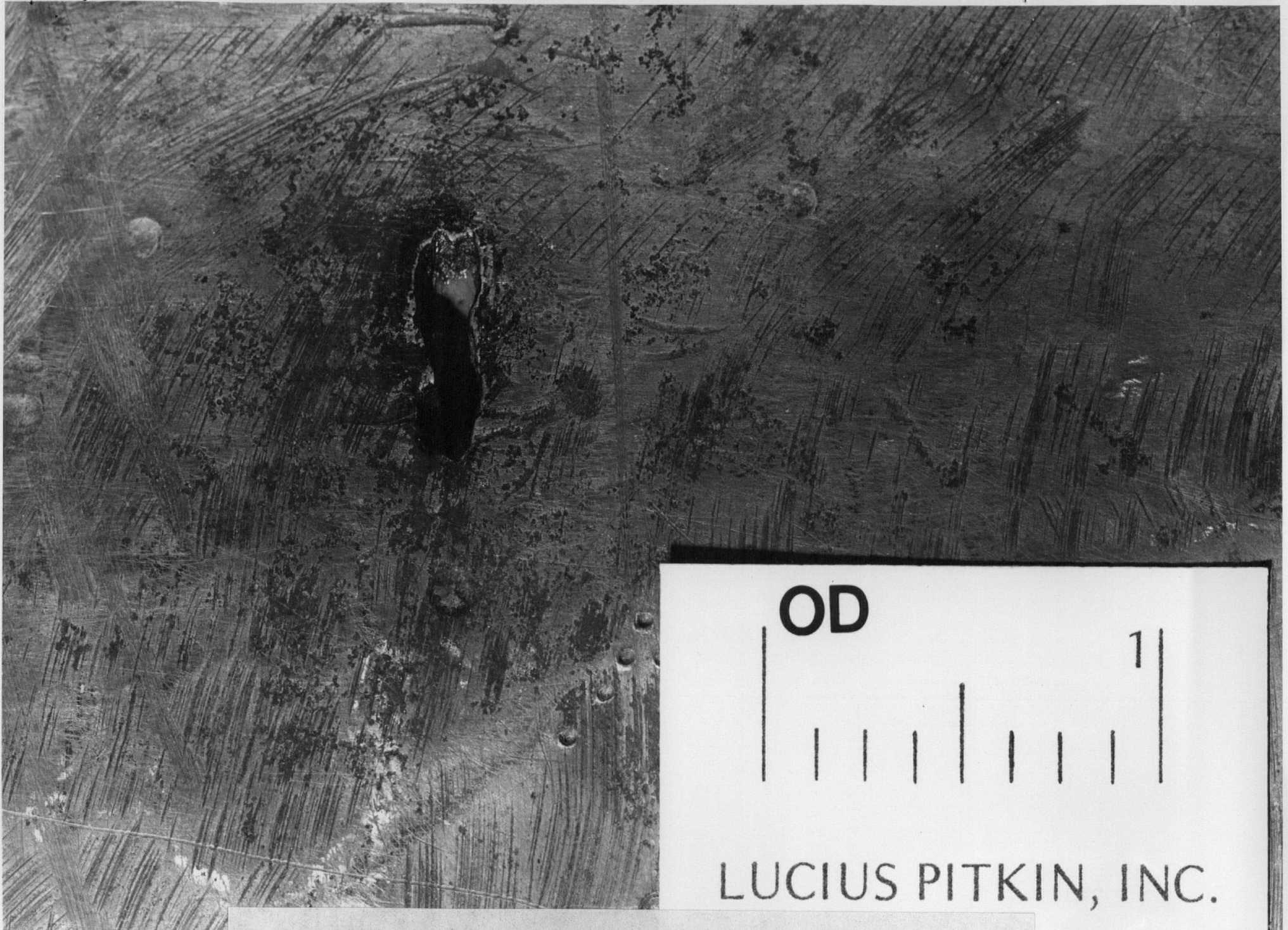


Fig. 7 THROUGH-THICKNESS DISCONTINUITY AT OUTER SURFACE

Lucius Pitkin
incorporated



Fig. 8

INNER SURFACE CRACKS OBSERVED WITH FLUORESCENT
MAGNETIC-PARTICLE UNDER ULTRAVIOLET LIGHT

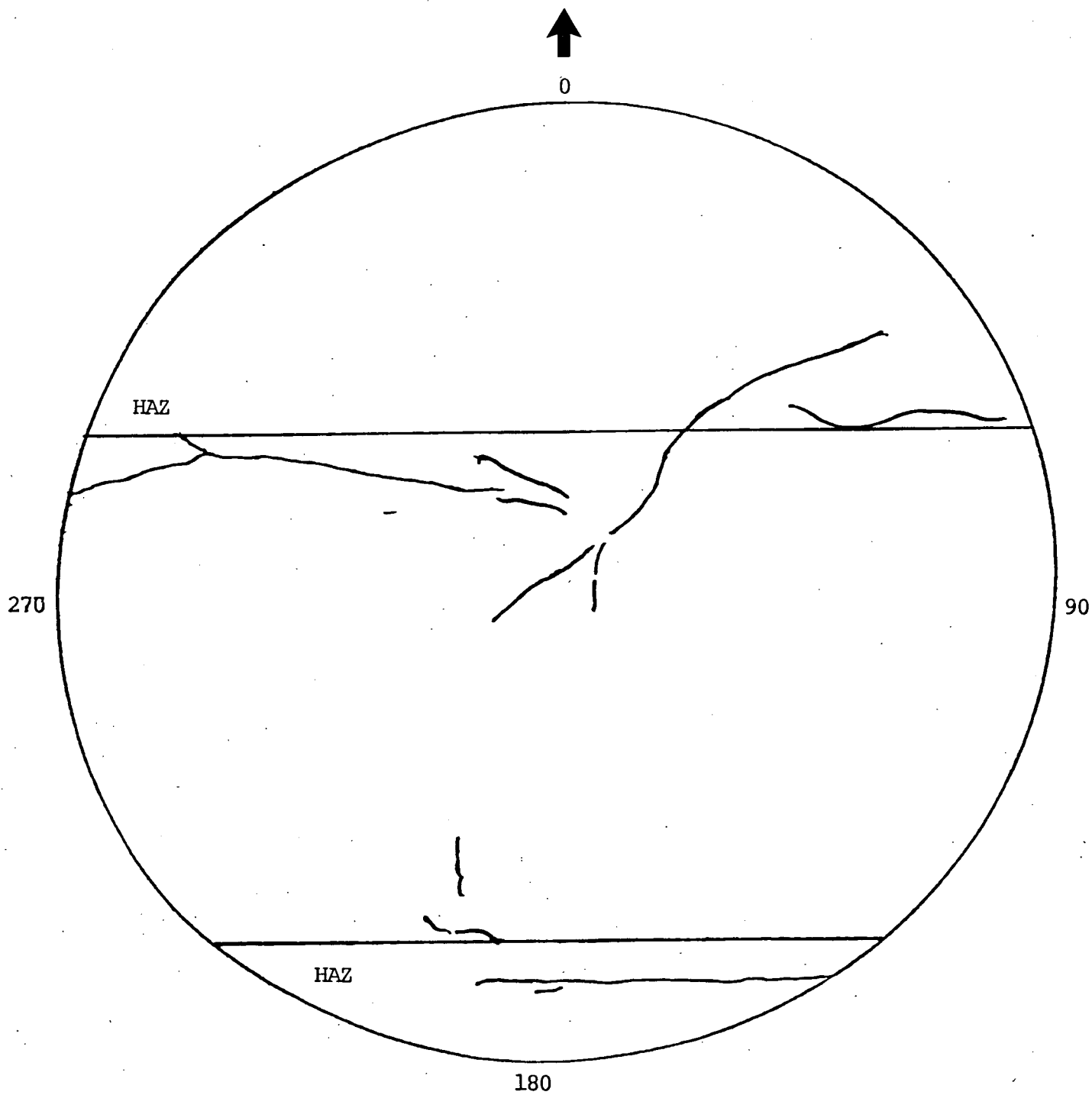


Fig. 8A INNER SURFACE CRACKS AS REVEALED BY FLUORESCENT MAGNETIC PARTICLE EXAMINATION

Lucius Pitkin
incorporated

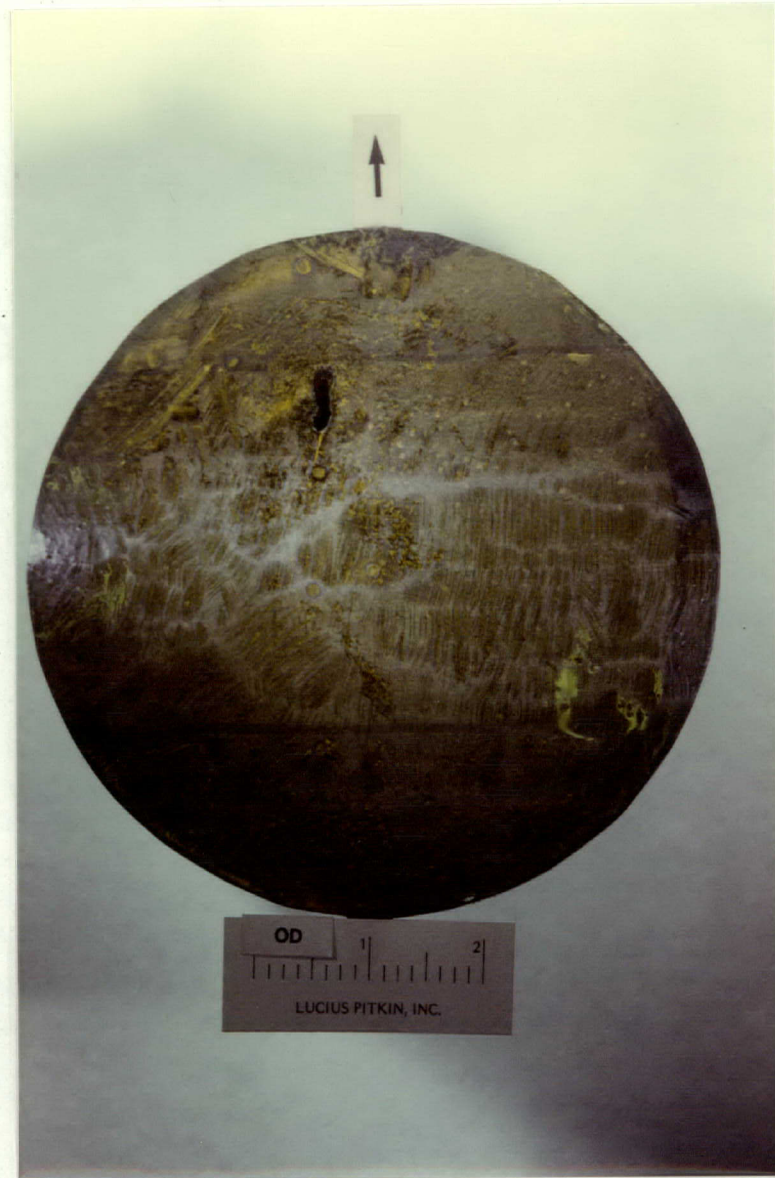


Fig. 9

OUTER SURFACE CRACK OBSERVED WITH FLUORESCENT
MAGNETIC-PARTICLE UNDER ULTRAVIOLET LIGHT

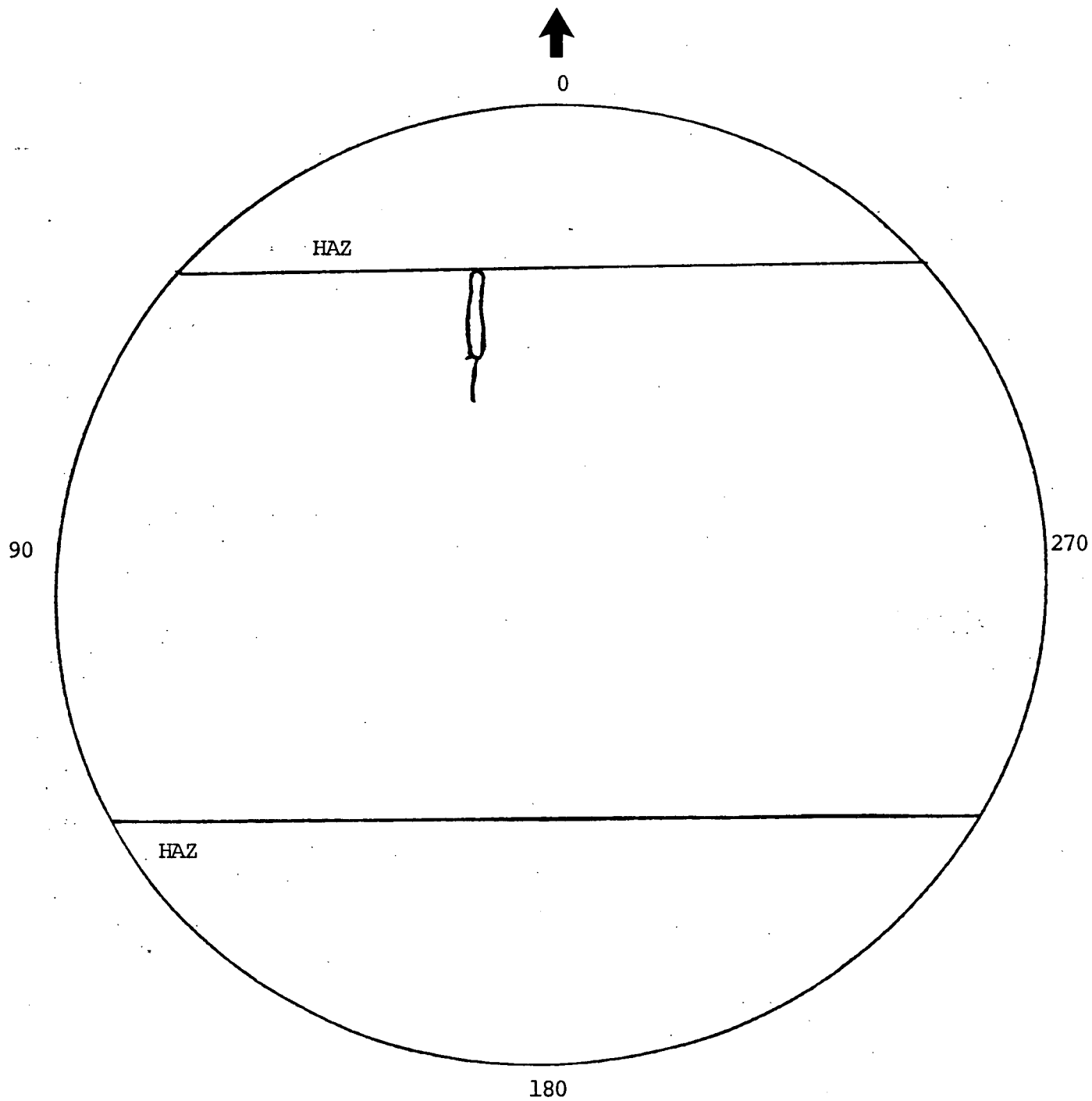


Fig. 9A OUTER SURFACE CRACKS AS REVEALED BY FLUORESCENT MAGNETIC PARTICLE EXAMINATION

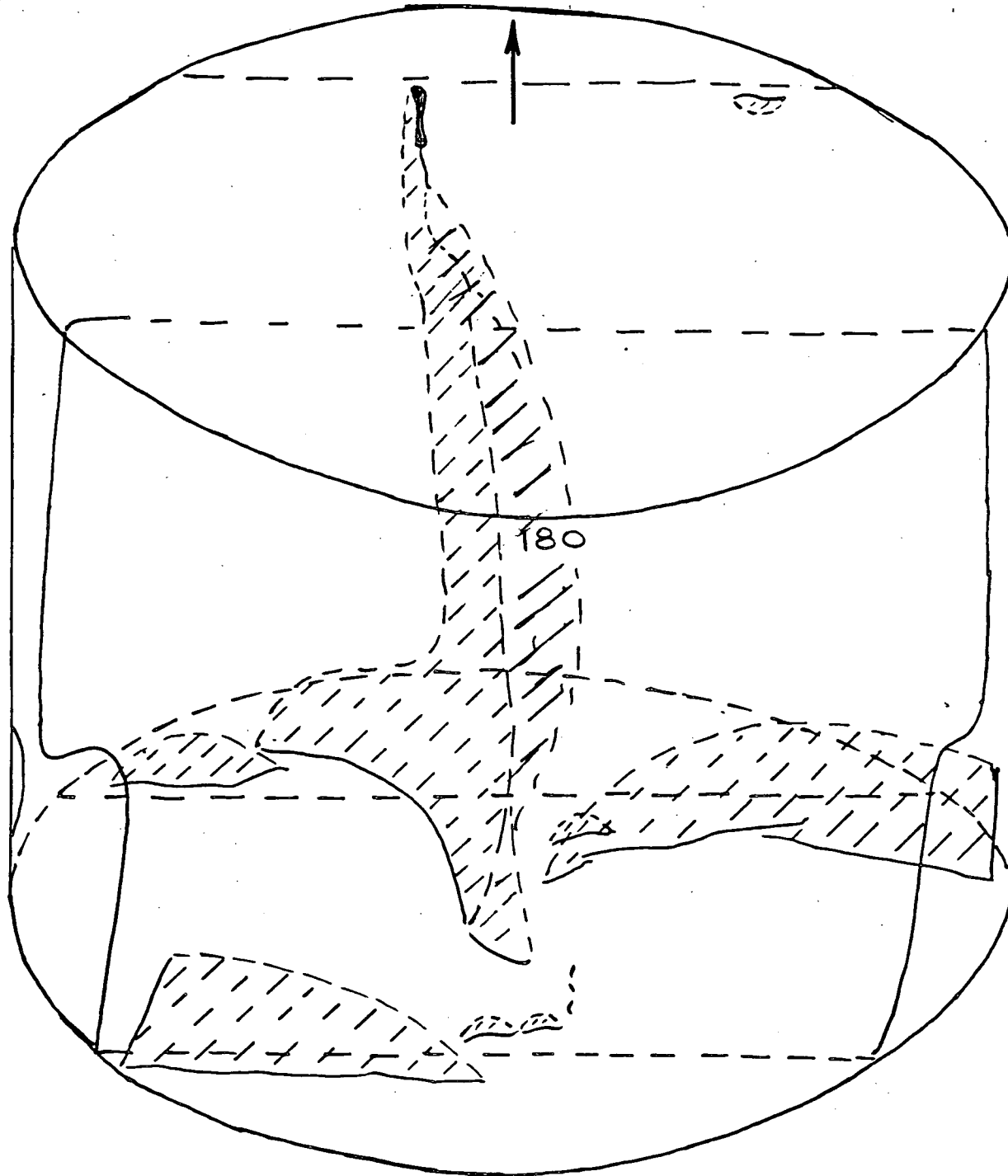


Fig. 10 NONDESTRUCTIVE EXAMINATION RESULTS OF 6-INCH DIAMETER
COUPON FROM UPPER SHELL TO CONE GIRTH WELD - SG32



Fig. 11 PERIPHERY OF 6-IN. DIAMETER COUPON - AFTER
LIGHT ETCHING

90°



270°

ID 180°

LUCIUS PITKIN, INC.

Fig. 12 PERIPHERY OF 6-IN. DIAMETER COUPON - AFTER LIGHT ETCHING

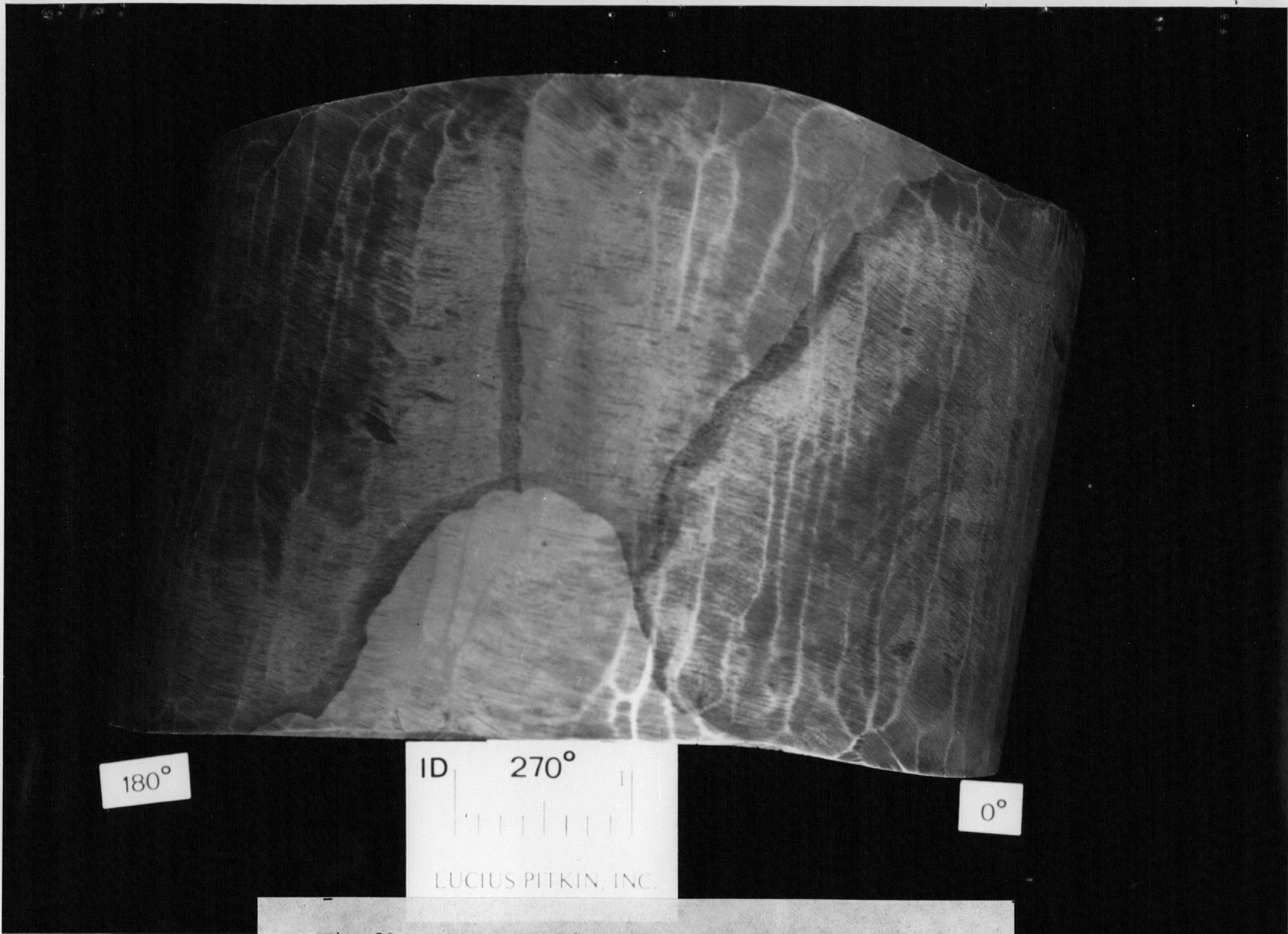


Fig. 13 PERIPHERY OF 6-IN. DIAMETER COUPON - AFTER
LIGHT ETCHING

270°

90°

ID 0° 1

LUCIUS PITKIN, INC.

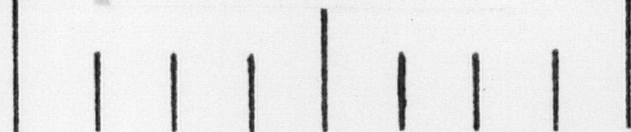
Fig. 14 PERIPHERY OF 6-IN. DIAMETER COUPON - AFTER LIGHT ETCHING



ID

270°

1



LUCIUS PITKIN, INC.

FIG. 15 PHOTOMACROGRAPH SHOWING ONE OF THE INNER SURFACE
CRACKS WHICH HAD EXTENDED INTO THE PERIPHERY OF THE COUPON

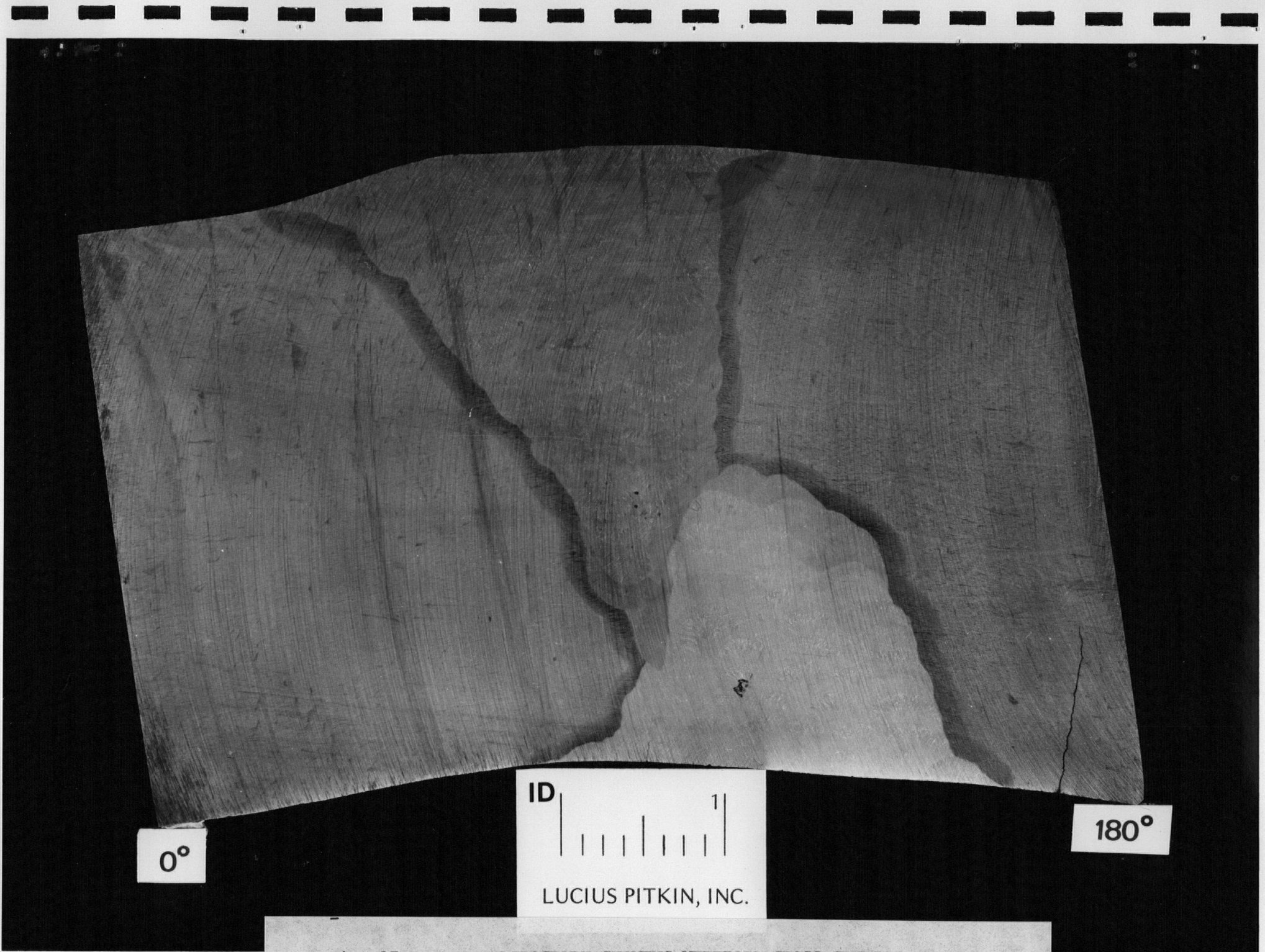
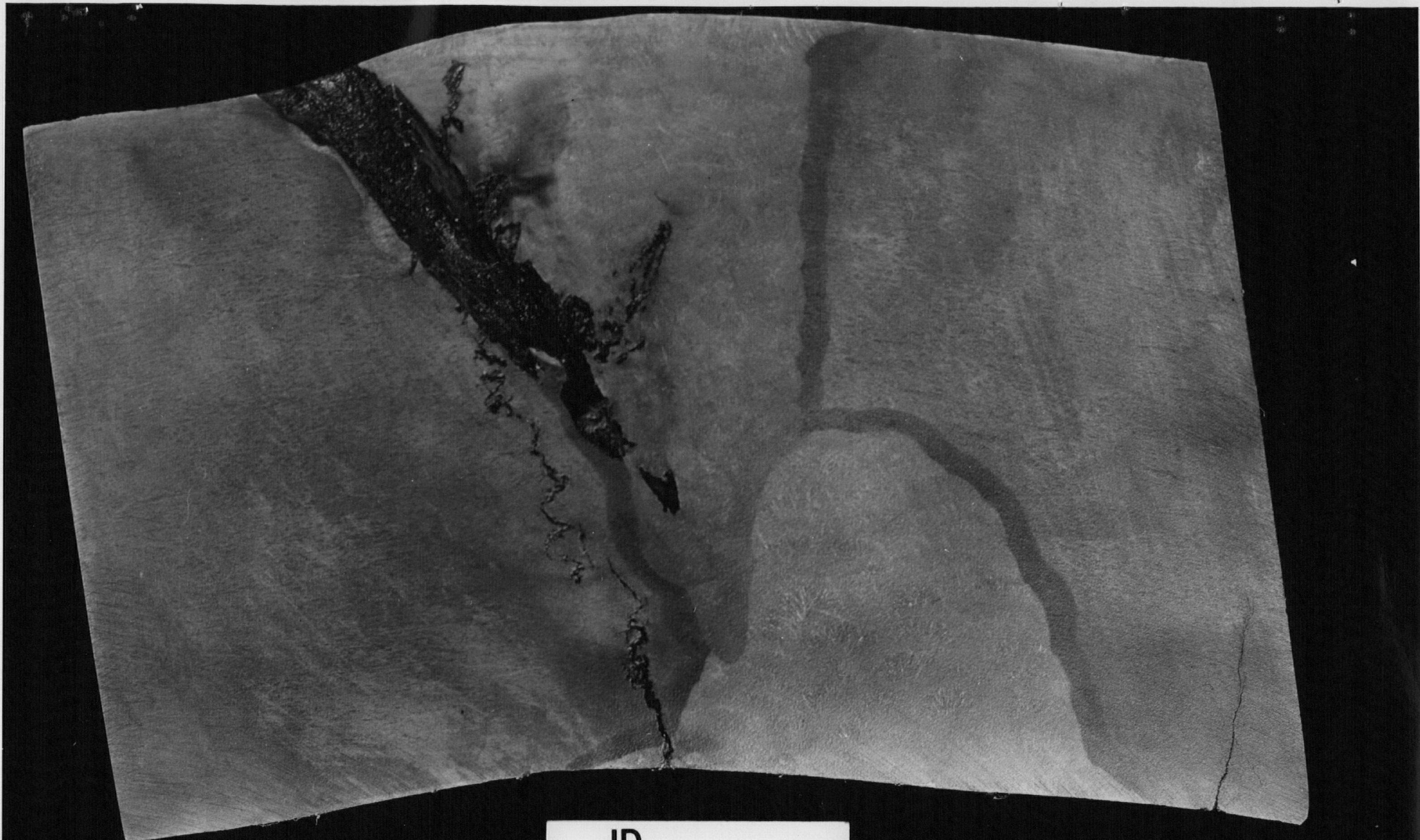
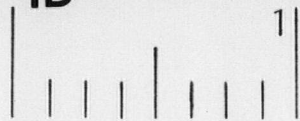


Fig. 17 PHOTOMACROGRAPH SHOWING VERTICAL CROSS-SECTION MATING TO THAT SHOWN IN FIG. 16



ID



1

LUCIUS PITKIN, INC.

Fig. 18 PHOTOMACROGRAPH OF VERTICAL CROSS-SECTION ADJACENT AND SLIGHTLY THROUGH THROUGH-WALL DISCONTINUITY



ID



Fig. 19

PHOTOMACROGRAPH SIMILAR TO THAT SHOWN IN FIG. 18 EXCEPT
AFTER ADDITIONAL GRINDING OF APPROXIMATELY 1/16 INCH

Lucius Pitkin
incorporated



Fig. 20

COLOR PHOTOMACROGRAPH OF VERTICAL CROSS-SECTION
INTERSECTING THROUGH-THICKNESS DISCONTINUITY

Lucius Pitkin
incorporated

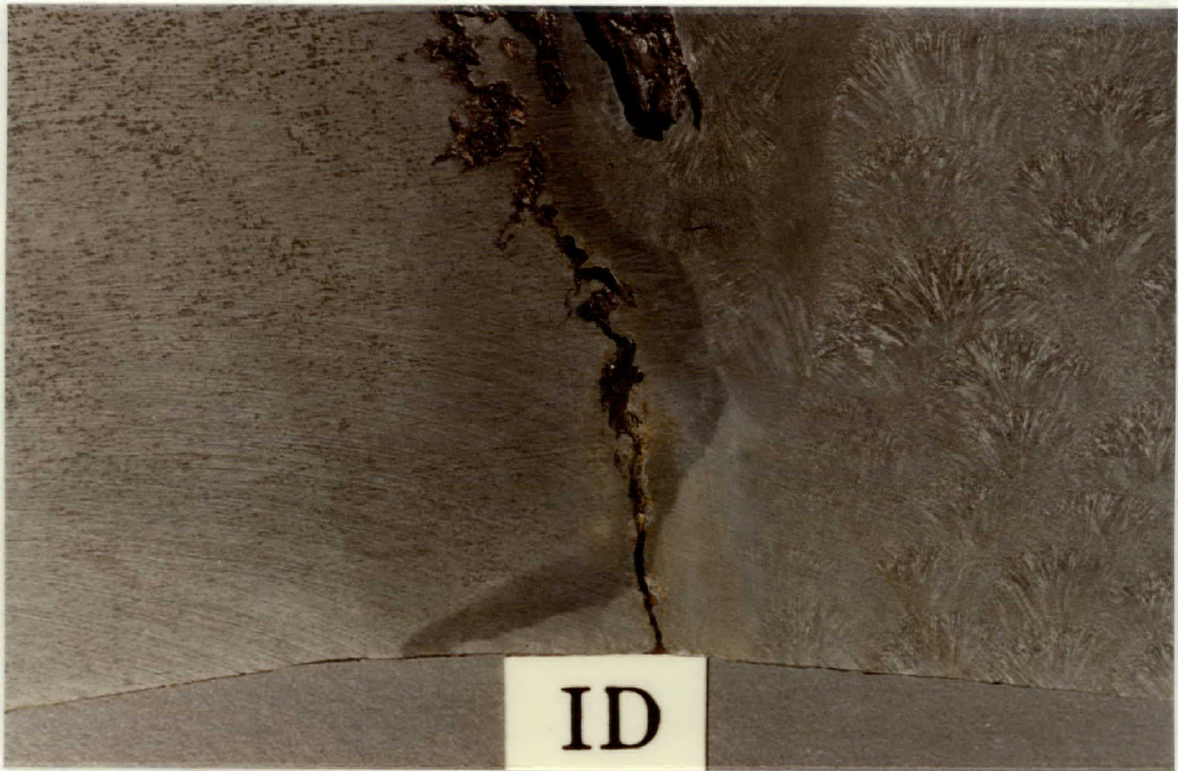


Fig. 21 PHOTOMACROGRAPH SHOWING WOOD FIBERS AND COPPER WITHIN THROUGH-THICKNESS DISCONTINUITY AT INNER SURFACE. WOOD FIBERS ARE THE RESULT OF THE INSERTION OF A WOODEN PLUG AFTER SHUTDOWN OF THE STEAM GENERATOR

**Lucius Pitkin
incorporated**

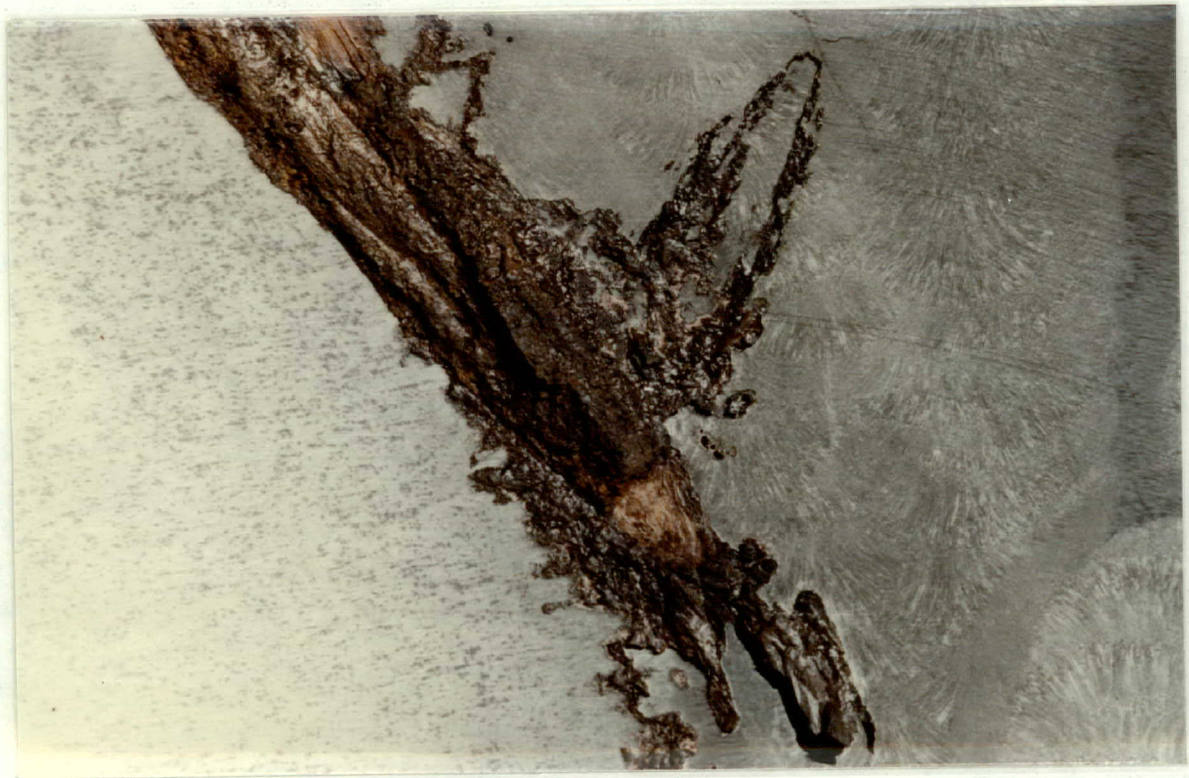


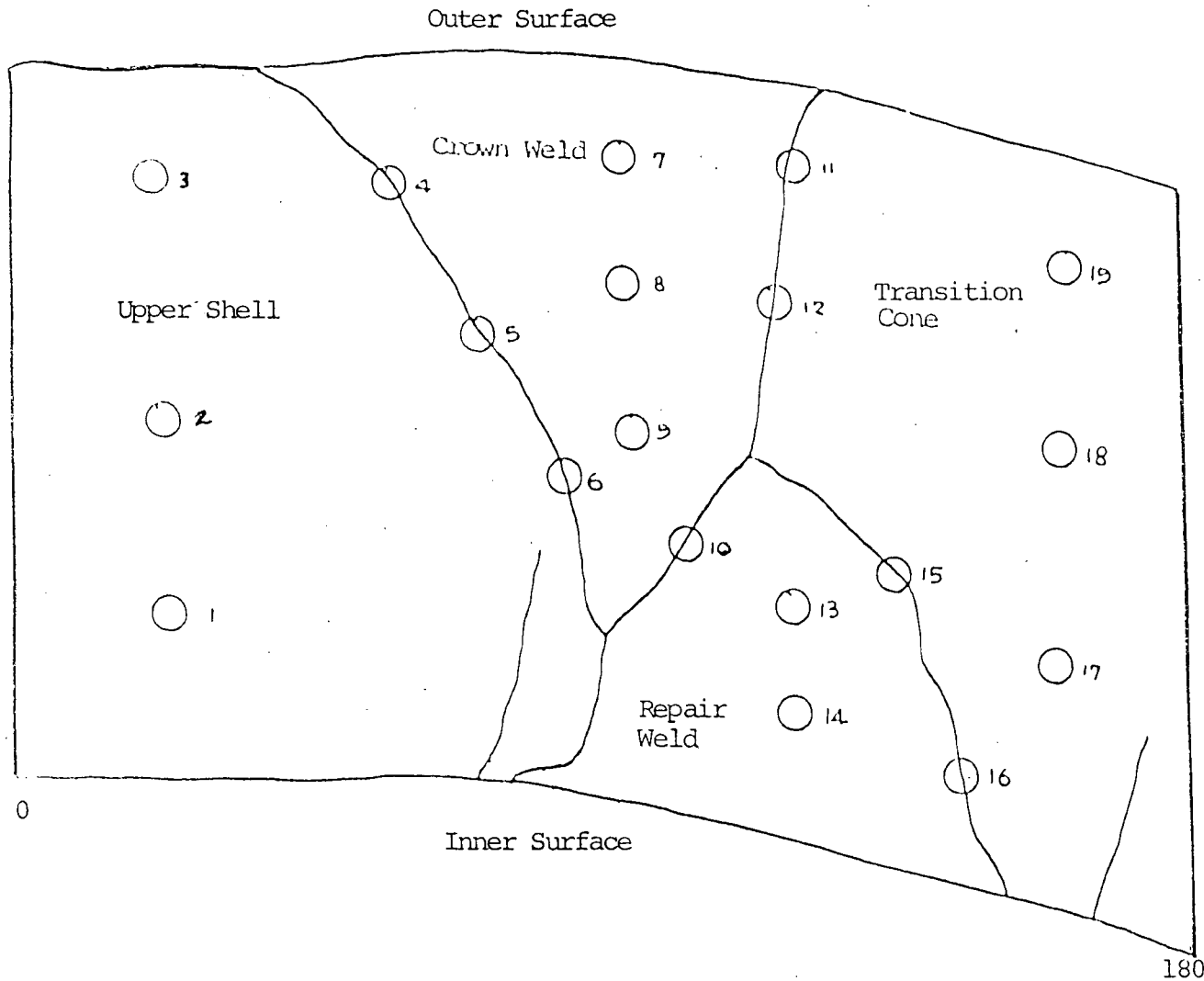
Fig. 22 PHOTOMACROGRAPH SHOWING WOOD FIBERS AND COPPER WITHIN
THROUGH-THICKNESS DISCONTINUITY AT ABOUT MID-WALL

Lucius Pitkin
incorporated



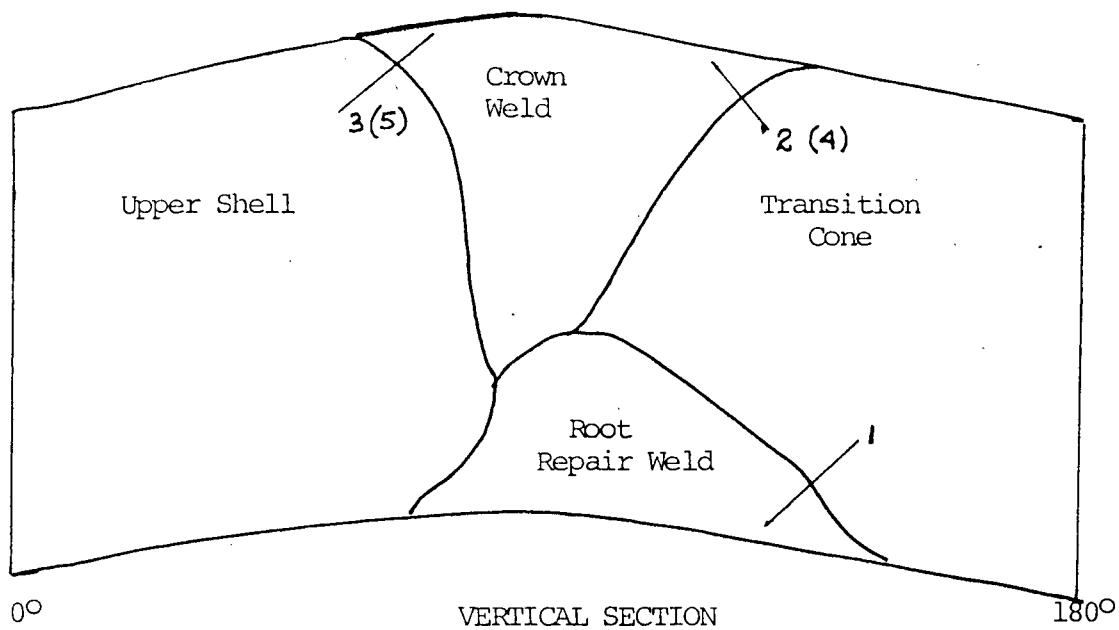
Fig. 23 PHOTOMACROGRAPH SHOWING WOOD FIBERS AND COPPER WITHIN
THROUGH THICKNESS DISCONTINUITY NEAR OUTER SURFACE

Lucius Pitkin
incorporated



Location	BHN	Approximate Tensile Strength, psi
1	187	90,000
2	187	90,000
3	197	94,000
4	255	120,000
5	255	120,000
6	229	108,000
7	207	99,000
8	217	103,000
9	229	109,000
10	217	103,000
11	229	109,000
12	241	116,000
13	197	94,000
14	187	90,000
15	229	108,000
16	217	103,000
17	197	94,000
18	192	92,000
19	197	94,000

Fig. 24 BRINELL HARDNESS SURVEY (3000 KG) VERTICAL CROSS-SECTION THROUGH GIRTH WELD, S.G. 32



KNOOP MICROHARDNESS SURVEY
(500 gm load)

<u>As Received</u>		<u>As Received</u>		<u>As Received</u>		<u>1000 F, 1 Hr.</u>		<u>1100 F, 1 Hr.</u>	
<u>1</u>		<u>2</u>		<u>3</u>		<u>(4)</u>		<u>(5)</u>	
<u>Location</u>	<u>Hardness</u>	<u>Location</u>	<u>Hardness</u>	<u>Location</u>	<u>Hardness</u>	<u>Location</u>	<u>Hardness</u>	<u>Location</u>	<u>Hardness</u>
Weld	23 RC	Weld	100 RB	Weld	20 FC	Weld	95 RB	Weld	95 RB
Weld	23 RC	Weld	99 RB	Weld	20 RC	Weld	95 RB	Weld	96 RB
HAZ	27 RC	HAZ	35 RC	HAZ	30 RC	HAZ	32 RC	HAZ	29 RC
HAZ	42 RC	HAZ	41 RC	HAZ	36 RC	HAZ	31 RC	HAZ	29 RC
HAZ	41 RC	HAZ	37 RC	HAZ	36 RC	HAZ	30 RC	HAZ	28 RC
HAZ	33 RC	HAZ	33 RC	HAZ	34 RC	HAZ	32 RC	HAZ	29 RC
HAZ	36 RC	HAZ	37 RC	HAZ	39 RC				
HAZ	29 RC	HAZ	35 RC	HAZ	34 RC				
Base Metal	98 RB	Base Metal	92 RB	Base Metal	97 RB	Base Metal	96 RB	Base Metal	95 RB
Base Metal	97 RB	Base Metal	94 RB	Base Metal	98 RB	Base Metal	95 RB	Base Metal	92 RB

Fig. 25 KNOOP MICROHARDNESS SURVEY (CONVERTED TO ROCKWELL.) AS-RECEIVED AND LABORATORY HEAT-TREATED SPECIMENS

**Lucius Pitkin
incorporated**



Fig. 25A

HEAT-AFFECTED ZONE MICROSTRUCTURE

400 X

Photomicrograph showing the general microstructure exhibited by the heat-affected zone between crown weld/upper shell. The heat-affected zone microstructure consists of lightly tempered martensite. The hardness of the heat-affected zone shown here was Rockwell C 41-42.

**Lucius Pitkin
incorporated**



Fig. 25B

HEAT-AFFECTED ZONE MICROSTRUCTURE - 400 X
1000 F ONE HOUR

Photomicrograph showing the heat-affected zone microstructure exhibited by the crown weld/upper shell after laboratory heat treating at 1000 F for one hour. The microstructure shown here consists of uniformly tempered martensite and had a hardness of Rockwell C 31-32.

**Lucius Pitkin
incorporated**



Fig. 25C

HEAT-AFFECTED ZONE MICROSTRUCTURE -
1100 F ONE HOUR

400 X

Photomicrograph showing the heat-affected zone microstructure exhibited by the crown weld/upper shell after laboratory heat treating at 1100 F for one hour. The microstructure shown here consists of uniformly tempered martensite and fine carbides and had a hardness of Rockwell C 28-29.

Lucius Pitkin
incorporated

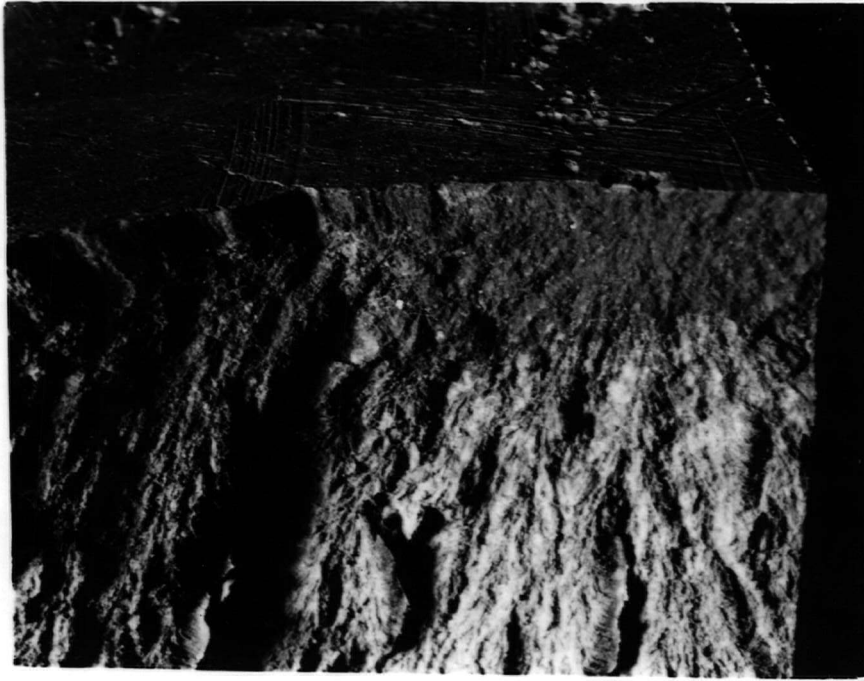


Fig. 26

FRACTURE SURFACE OF OPENED-UP CRACK AT
INNER SURFACE OF COUPON

4 X

Close-up photograph showing the fracture surface of opened-up crack which initiated at the inner surface of the steam generator coupon. It can be seen that the fracture is associated with fine pits on the inner surface.

Lucius Pitkin
incorporated

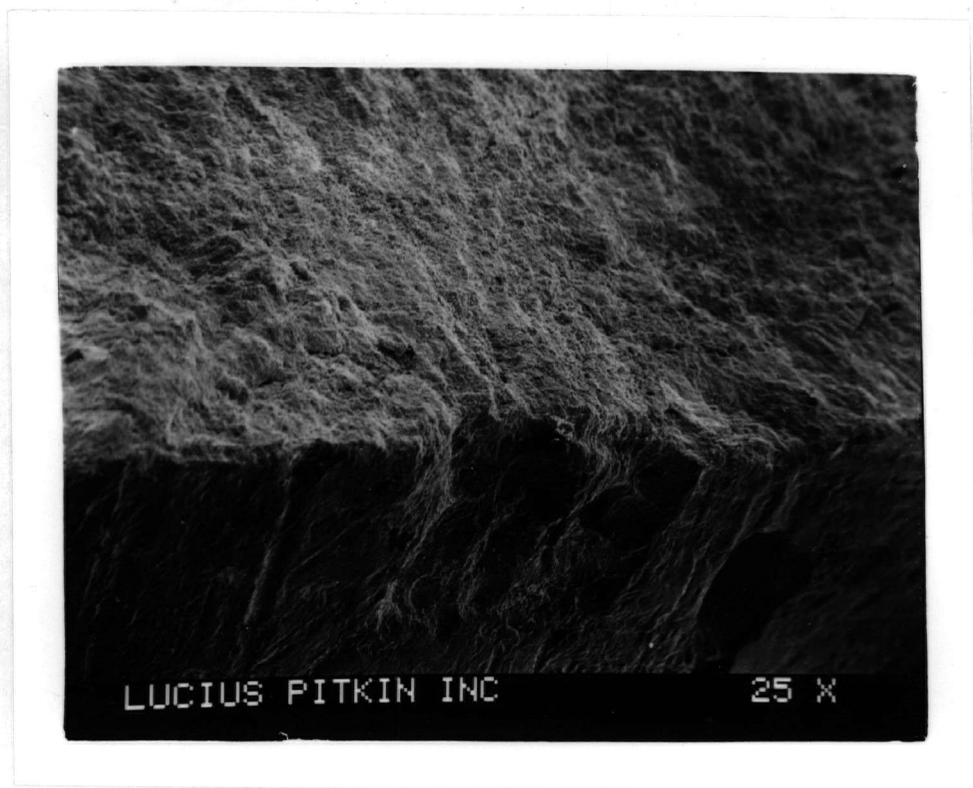


Fig. 27

SCANNING ELECTRON MICROGRAPH
OF CRACK SURFACE

25 X

Scanning electron micrograph showing the corroded fracture surface of crack which initiated at the inner surface of the steam generator coupon.

**Lucius Pitkin
incorporated**

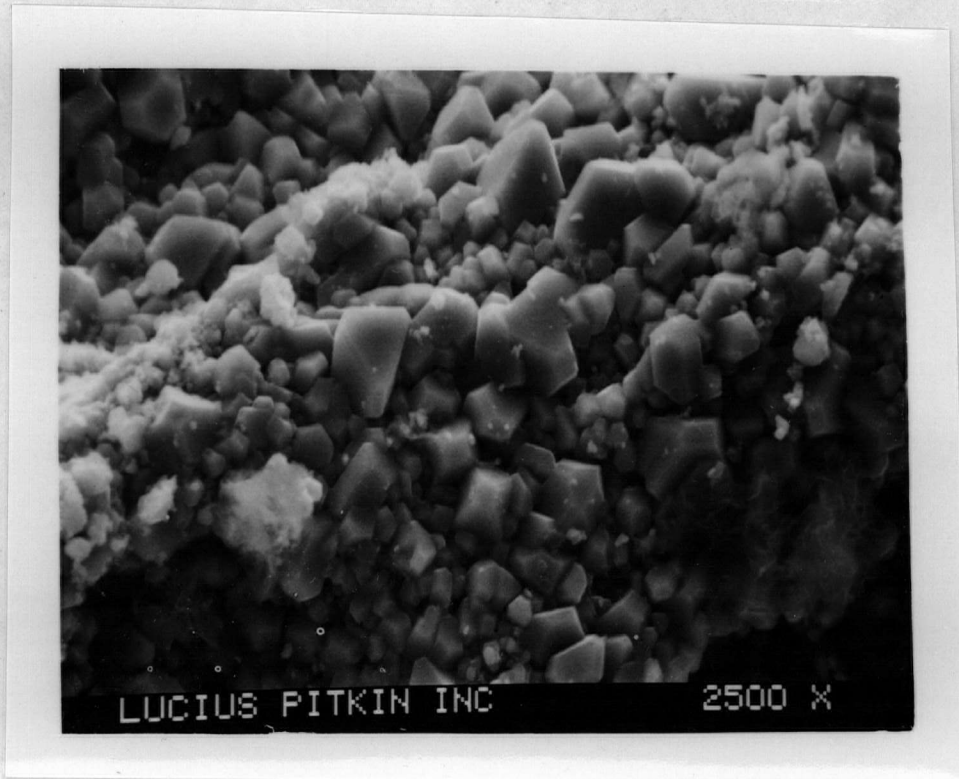


Fig. 28

CRACK FRACTURE SURFACE OXIDE

2500 X

Scanning electron micrograph showing discrete crystals of iron oxide present on the crack fracture surface. The presence of these iron oxide crystals is indicative of the presence of oxygen in the secondary water system.

Lucius Pitkin
incorporated



Fig. 29

CRACK FRACTURE SURFACE
AFTER CLEANING

25 X

SEM similar to that shown in Fig. 27, except after extensive cleaning to remove surface oxide. It can be seen that the fracture surface is generally smooth as is characteristic of progressive or fatigue cracking, but no striations could be found.

Lucius Pitkin
incorporated



Fig. 30 CRACK FRACTURE SURFACE BELOW INNER SURFACE 250 X

Scanning electron micrograph showing the oxide covered crack fracture surface approximately 1/2 in. from the inner surface of the coupon. The somewhat radially ridged appearance of the fracture surface indicates the fracture to be the result of progressive or fatigue cracking.

Lucius Pitkin
incorporated

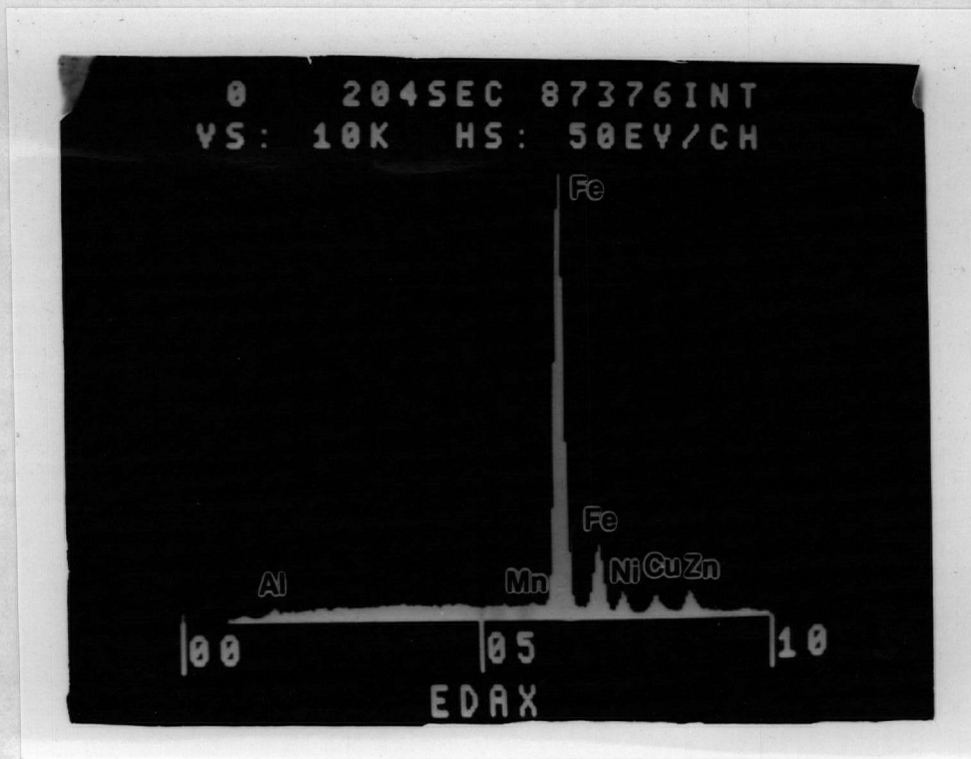


Fig. 31

ENERGY DISPERSIVE X-RAY SPECTRUM

Energy dispersive X-ray spectrum of the fracture surface of one of the coupon cracks. The energy peaks of iron, manganese and nickel are attributed to the base metal whereas the copper and zinc energy peaks are attributable to carry over from copper alloy components in the secondary system.

**Lucius Pitkin
incorporated**



Fig. 32

CRACKS IN REPAIR WELD - INNER SURFACE

6 X

Photomicrograph showing one of the typical progressive or fatigue cracks, initiated near the toe of the repair weld, which propagated into the transition cone base material. It can also be seen that very fine, secondary cracks are present which emanate from fine pits in the surface of the repair weld metal.

Lucius Pitkin
incorporated



Fig. 33

CORROSION-FILLED CRACK IN REPAIR WELD

400 X

Photomicrograph showing corrosion-filled crack initiated from inner surface of repair weld.

Lucius Pitkin
incorporated

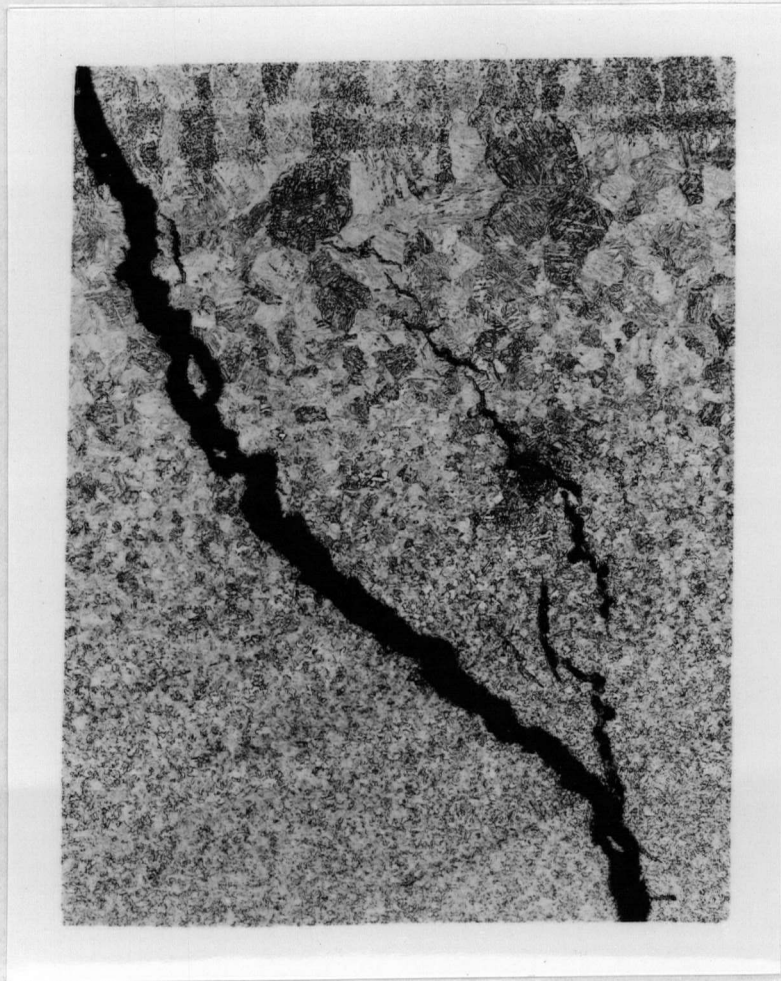


Fig. 34

PROGRESSIVE OR FATIGUE CRACKS IN REPAIR WELD

50 X

Photomicrograph showing typical progressive or fatigue cracks which had initiated from the inner surface of the repair weld and had propagated through the heat-affected zone into the transition cone base metal. It can be seen that the cracks are slightly branching and transgranular.

Lucius Pitkin
incorporated



Fig. 35

HEAT-AFFECTED ZONE CRACKS

200 X

Photomicrograph showing the oxide-filled transgranular nature of the heat-affected zone cracks observed in the girth weld coupon.

The general microstructure shown here consists of coarse, lightly tempered martensite.

Lucius Pitkin
incorporated

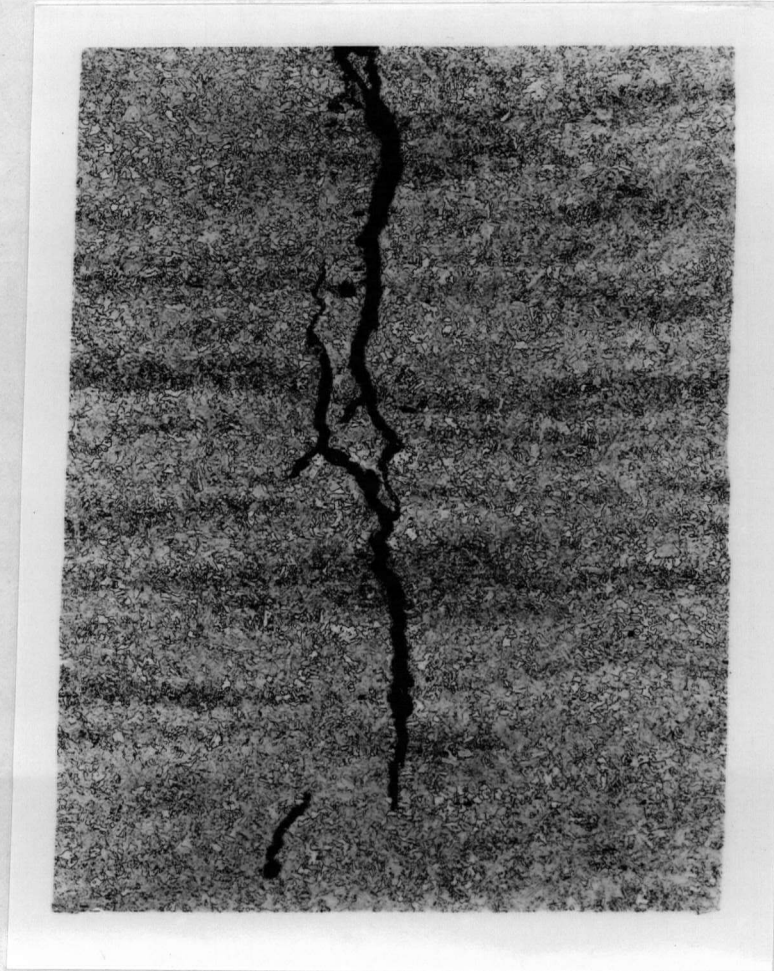


Fig. 36

TRANSITION CONE BASE METAL CRACKS

50 X

Photomicrograph showing the transgranular nature exhibited by the progressive or fatigue cracks which had propagated into the transition cone base metal.

The general microstructure of the transition cone consists of pearlite and ferrite, a structure characteristic of SA 302B material.

Lucius Pitkin
incorporated



Fig. 37

INNER SURFACE CRACKS IN TRANSITION CONE

6 X

Photomicrograph showing progressive or fatigue crack emanating from corrosion pit at the inner surface of transition cone base material.

Lucius Pitkin
incorporated

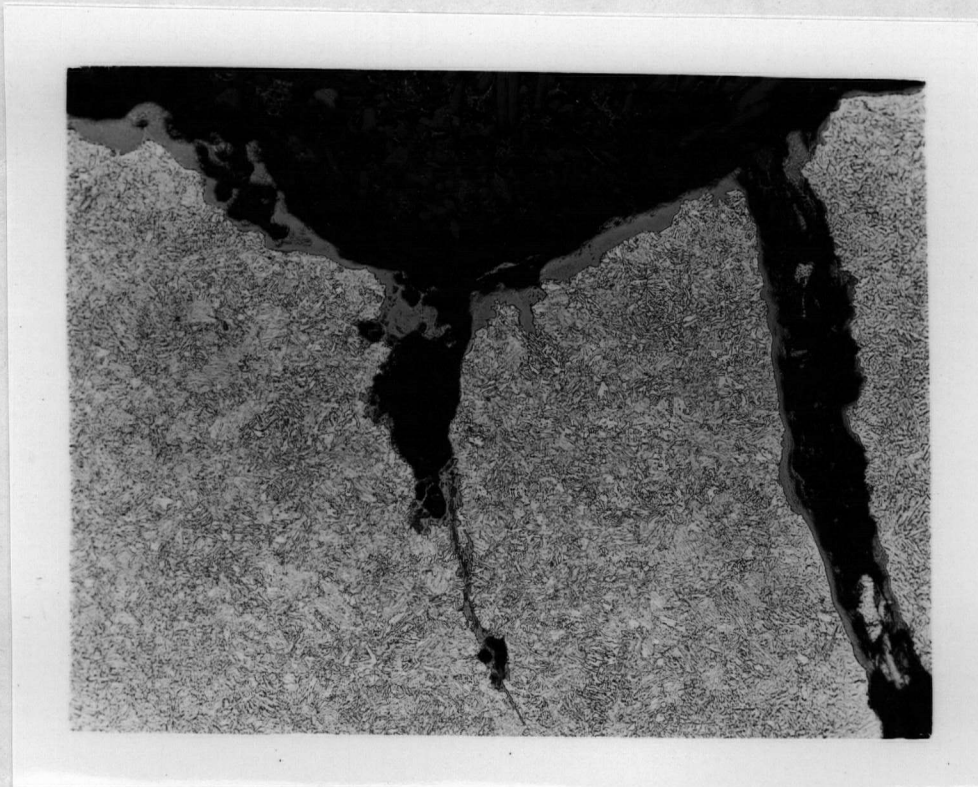


Fig. 38 INNER SURFACE CRACKS IN TRANSITION CONE 100 X

Photomicrograph similar to that shown in Fig. 37 except at higher magnification more clearly showing the corrosion-filled transgranular fatigue cracks which initiated from an inner surface pit.

Lucius Pitkin
incorporated

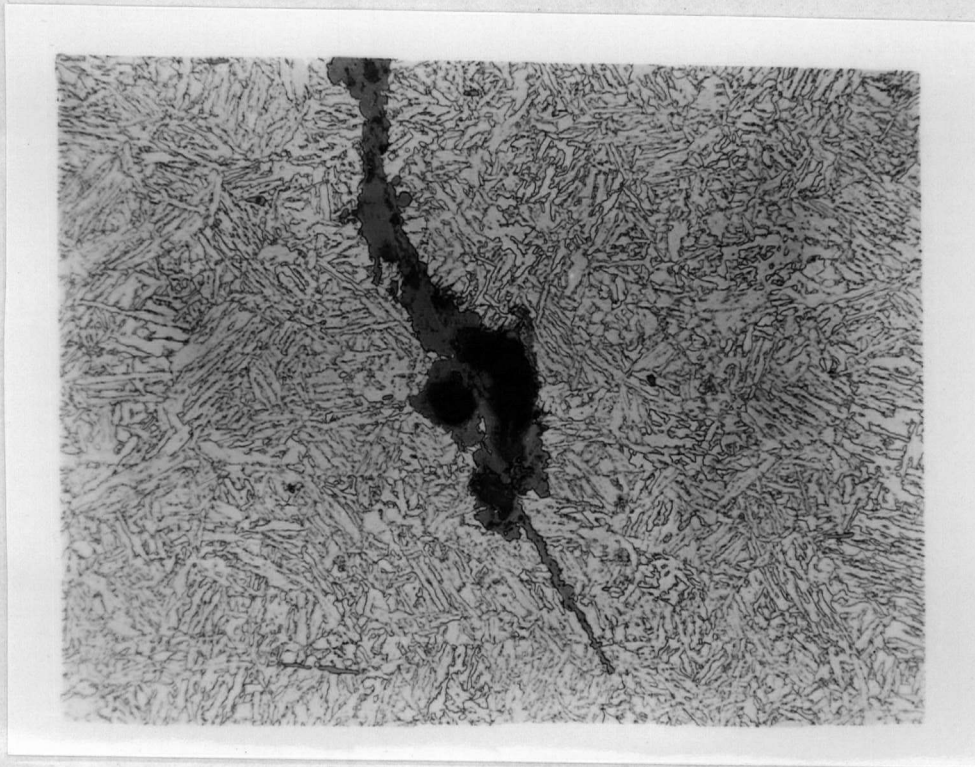


Fig. 39

CORROSION-FILLED CRACK - TRANSITION CONE

400 X

Photomicrograph showing the tip of the progressive or fatigue crack shown in Figs. 37 and 38. It can be seen that the crack is corrosion filled and transgranular as is typical of progressive or fatigue cracking.

**Lucius Pitkin
incorporated**

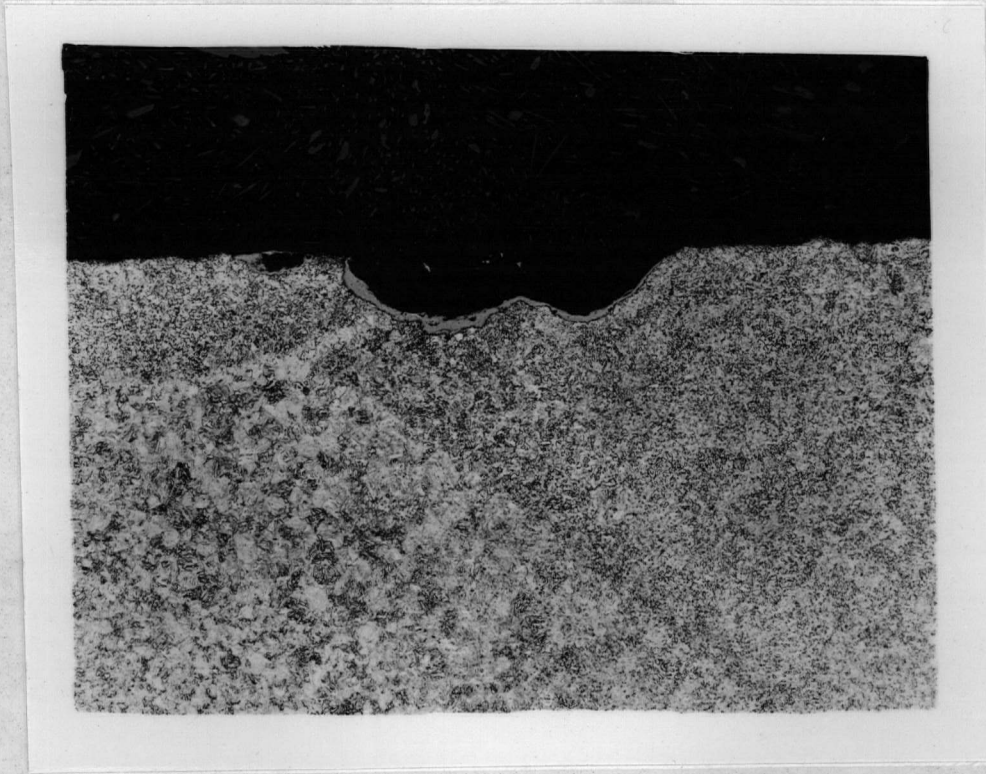


Fig. 39A

INNER SURFACE PITS

50 X

Photomicrograph showing the presence of fine pits on the inner surface of the coupon near the heat-affected zone.

Lucius Pitkin
incorporated

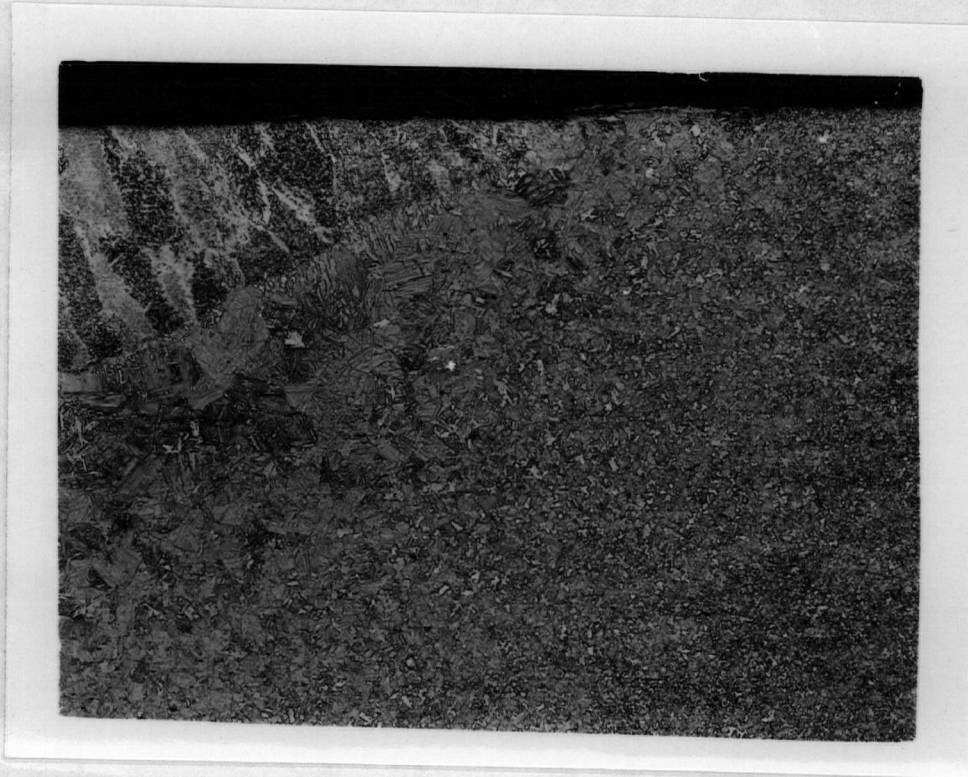


Fig. 40

REPAIR WELD/TRANSITION CONE
HEAT-AFFECTED ZONE

50 X

Photomicrograph showing the general microstructure in the heat-affected zone between the repair weld and transition cone base material. The microstructure shown here consists of lightly tempered martensite.

Lucius Pitkin
incorporated

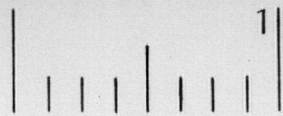
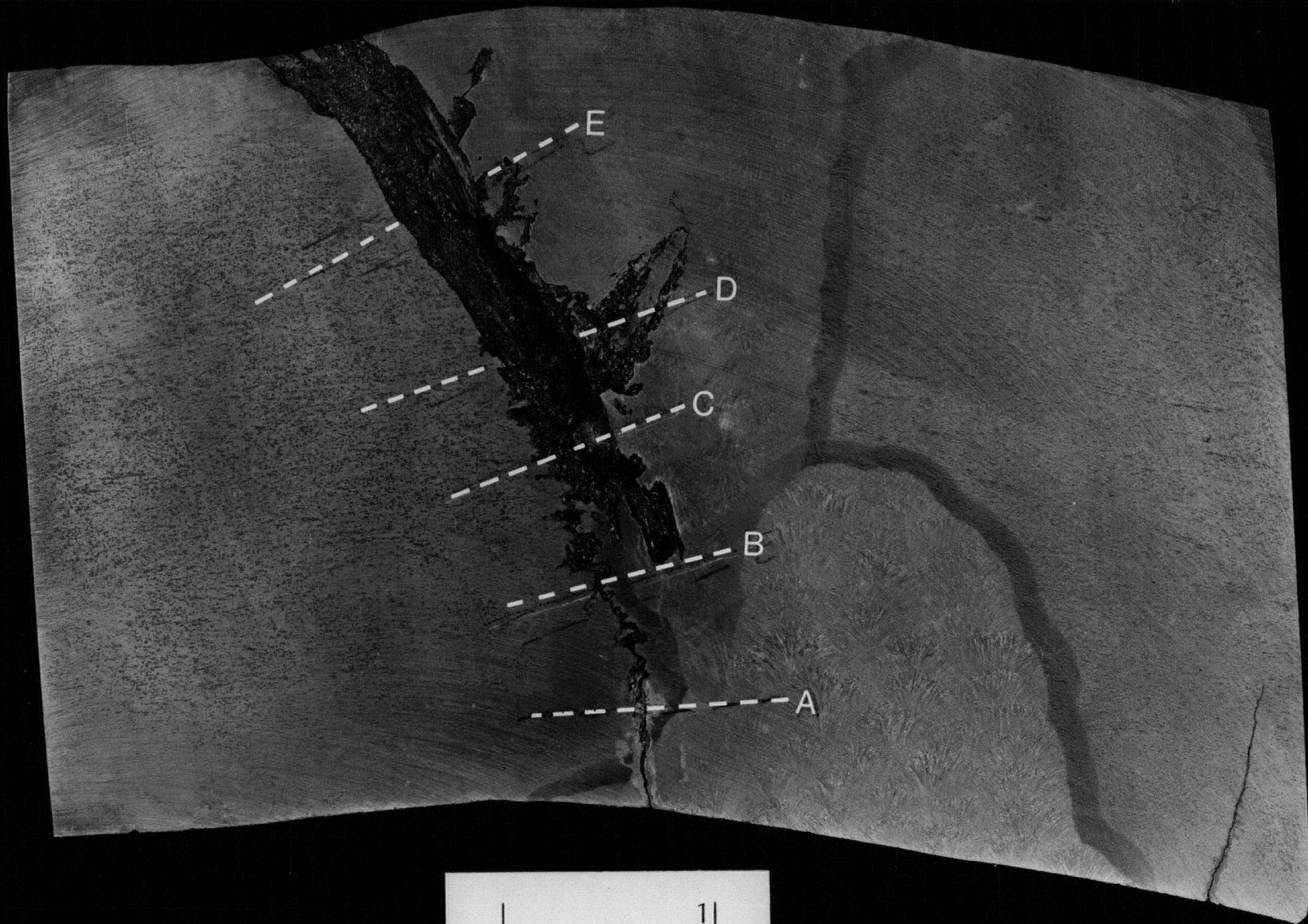


Fig. 41

HEAT-AFFECTED ZONE MICROSTRUCTURE

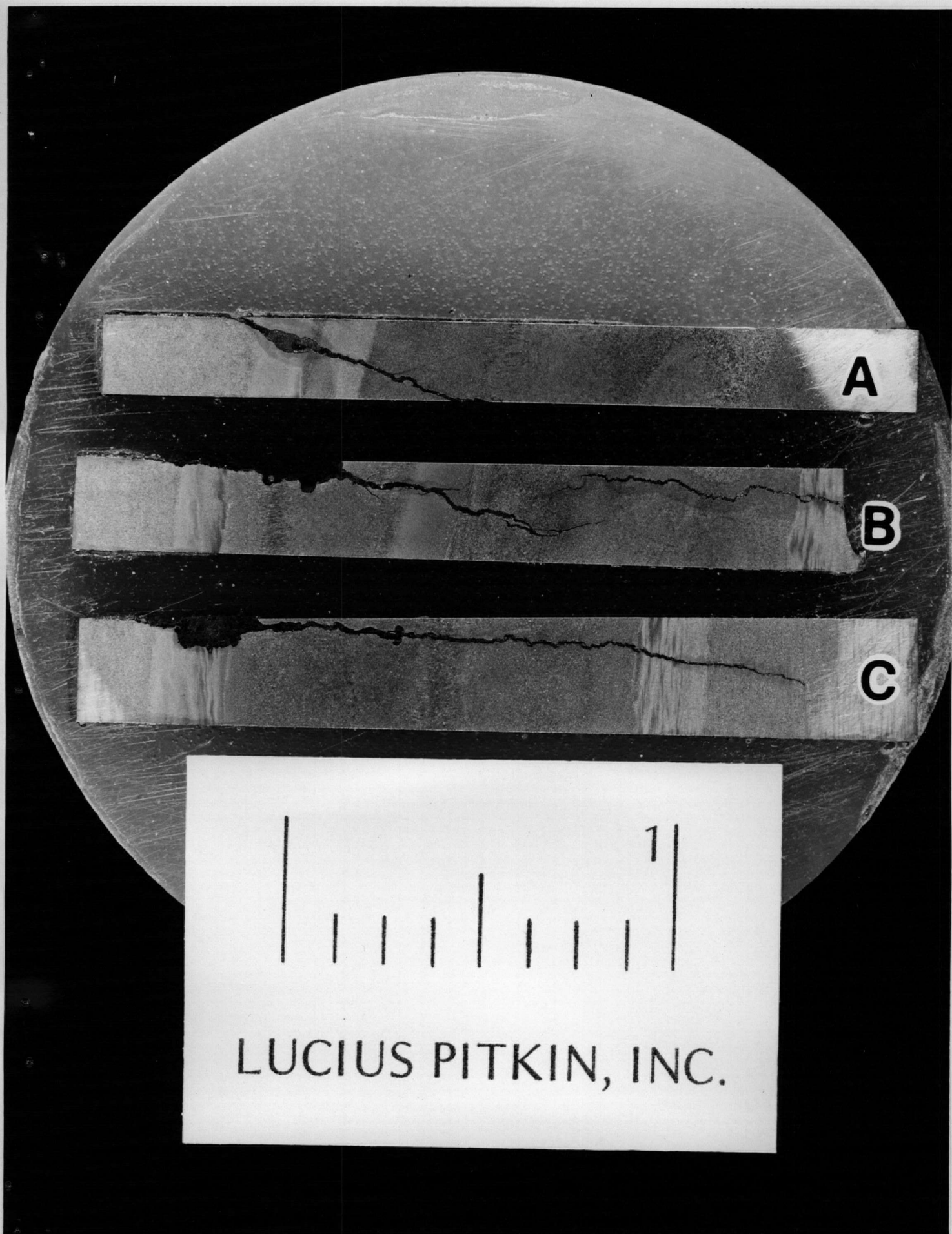
400 X

Photomicrograph similar to that shown in Fig. 40, except at higher magnification, showing the general microstructure exhibited by the heat-affected zone between repair weld and transition cone. The heat-affected zone microstructure consists of lightly tempered martensite.



LUCIUS PITKIN, INC.

Fig. 42 PHOTOGRAPH SHOWING THE LOCATION OF MICROSPECIMENS TAKEN THROUGH THROUGH-WALL DISCONTINUITY



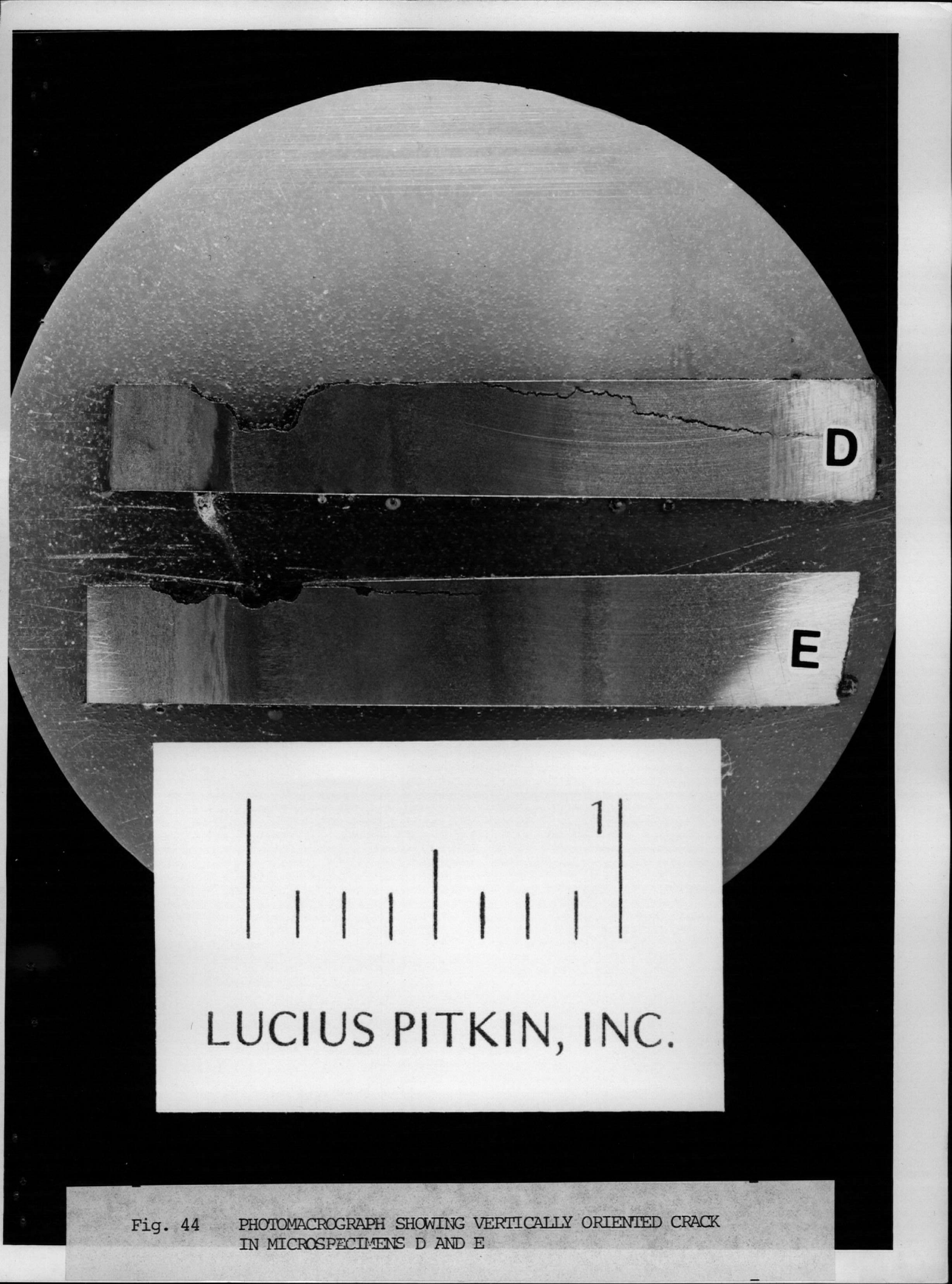
A

B

C

LUCIUS PITKIN, INC.

Fig. 43 PHOTOMACROGRAPH SHOWING VERTICALLY ORIENTED CRACK IN MICROSPECIMENS A THROUGH C



D

E

1

LUCIUS PITKIN, INC.

Fig. 44 PHOTOMACROGRAPH SHOWING VERTICALLY ORIENTED CRACK IN MICROSPECIMENS D AND E

Lucius Pitkin
incorporated

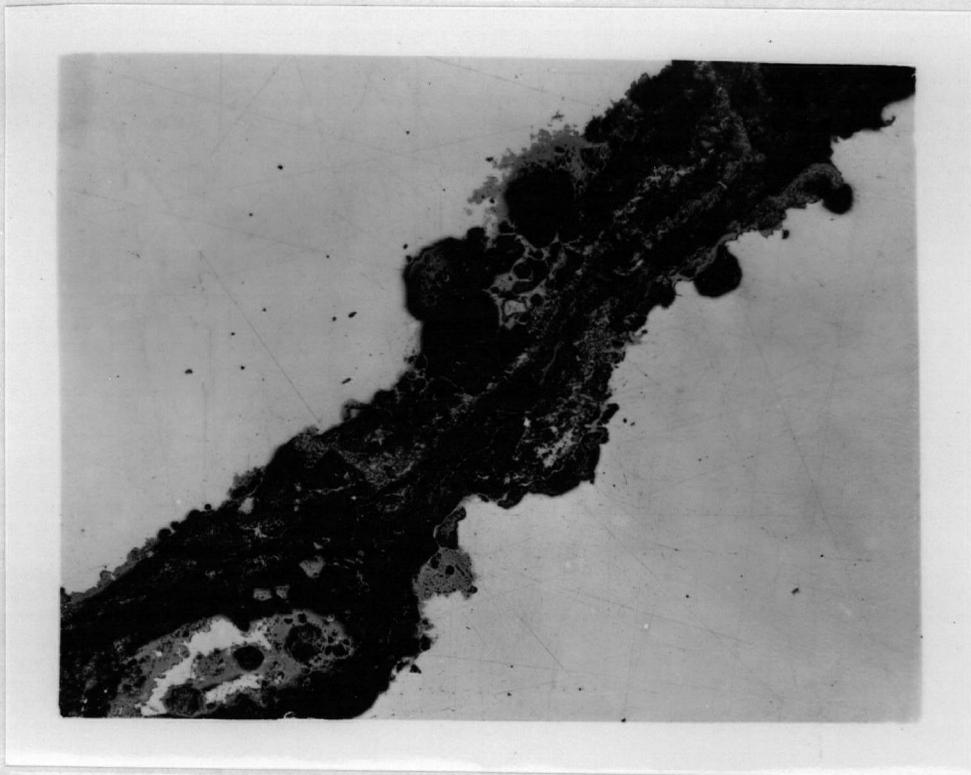


Fig. 45

THROUGH-WALL CRACK - AS POLISHED

100 X

Photomicrograph showing the oxide-filled vertically oriented through-wall crack. No evidence of weld defects such as slag or gross porosity is associated with the crack. The area shown here is from specimen B (Fig. 43).

Lucius Pitkin
incorporated

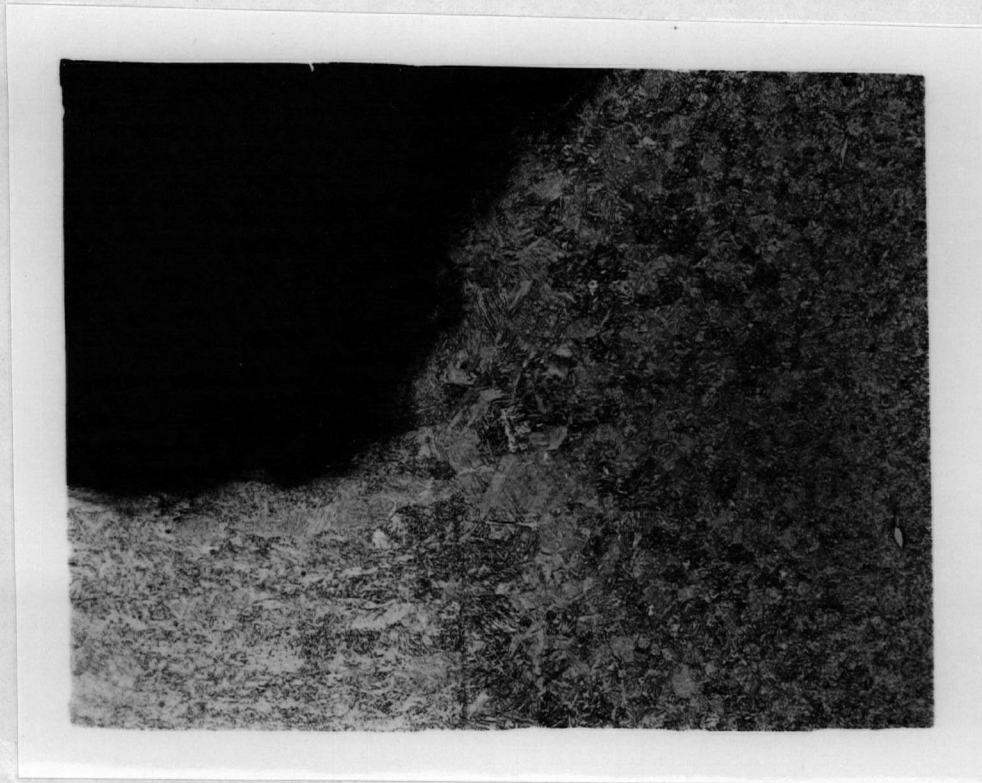


Fig. 46

THROUGH-WALL CRACK - HEAT-AFFECTED ZONE

50 X

Photomicrograph showing the vertically oriented through-wall crack in the area of upper shell/crown weld heat-affected zone. It can be seen that the crack profile is smooth and slightly eroded as would occur from steam/water escaping from the generator.

Lucius Pitkin
incorporated



Fig. 47

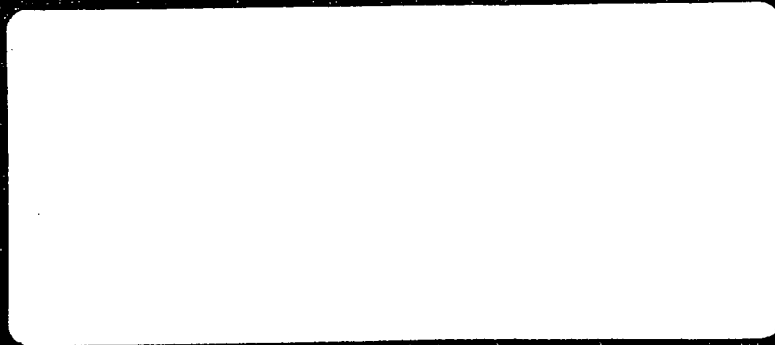
THROUGH-WALL CRACK

50 X

Photomicrograph showing the vertically oriented through-wall crack in the transition cone base metal. Here, as in Figs. 45 and 46, no welding defects are associated with the crack.

Lucius Pickin

INCORPORATED



EST. 1887

Metallurgical and Chemical Consultants
Casting Laboratories Nondestructive Examination Services

60 HUDSON STREET, NEW YORK, N.Y. 10013

— NOTICE —

THE ATTACHED FILES ARE OFFICIAL RECORDS OF THE DIVISION OF DOCUMENT CONTROL. THEY HAVE BEEN CHARGED TO YOU FOR A LIMITED TIME PERIOD AND MUST BE RETURNED TO THE RECORDS FACILITY BRANCH 016. PLEASE DO NOT SEND DOCUMENTS CHARGED OUT THROUGH THE MAIL. REMOVAL OF ANY PAGE(S) FROM DOCUMENT FOR REPRODUCTION MUST BE REFERRED TO FILE PERSONNEL.

DEADLINE RETURN DATE

50-286

11/17/82

8211220344

RECORDS FACILITY BRANCH